MATHEMATICAL MODELING, 3D DESIGN, CFD SIMULATION & DEVELOPMENT OF UAV

Wah Engineering College

GROUP MEMBERS

Aqsa Sheikh	UW-19-ME-BSc-001
M. Hassan Asif	UW-19-ME-BSc-019
M. Faheem Zia	UW-19-ME-BSc-053
M. Sarmad Inayat	UW-19-ME-BSc-057
Huzaifa Arfan Virk	UW-19-ME-BSc-073

Supervisor

Engr. Waqas Javid

Department of Mechanical Engineering

Wah Engineering College, Wah Cantt

PROJECT ID		NUMBER OF MEMBERS	05

TITLE	MATHEMATICAL MODELING, 3D DESIGN, CFD SIMULATION & DEVELOPMENT OF UAV

MEMBER NAME	REG #	EMAIL ADDRESS
Aqsa Sheikh	UW-19-ME-BSc-001	uw-19-me-bsc-001@wecuw.edu.pk
M. Hassan Asif	UW-19-ME-BSc-019	uw-19-me-bsc-019@wecuw.edu.pk
M. Faheem Zia	UW-19-ME-BSc-053	uw-19-me-bsc-053@wecuw.edu.pk
M. Sarmad Inayat	UW-19-ME-BSc-057	uw-19-me-bsc-057@wecuw.edu.pk
Huzaifa Arfan Virk	UW-19-ME-BSc-073	uw-19-me-bsc-073@wecuw.edu.pk

CHECKLIST

Number of pages attached with this form	
I/We have enclosed the soft-copy of this document along-with the codes and scripts created by ourselves	**YES / NO**
My/Our supervisor has attested the attached document	**YES / NO**

DECLARATION

We hereby declare that this project report is based on our original work except for citations and quotation which have been duly acknowledged. We also declare that it has not been previously and currently submitted for any degree award at Wah Engineering College or other institutions.

AUTHORS

Aqsa Sheikh

_____

Reg# UW-19-ME-BSc-001

M. Hassan Asif

_____

Reg # UW-19-ME-BSc-019

M. Faheem Zia

_____

Reg # UW-19-ME-BSc-053

M. Sarmad Inayat

_____

Reg # UW-19-ME-BSc-057

Huzaifa Arfan Virk

_____

Reg # UW-19-ME-BSc-073

CERTIFICATION

This is to certify that project entitled "Mathematical modelling, 3D design, CFD simulation & development of UAV" which is submitted in partial fulfilment of their requirement for the award of degree, Bachelor of Mechanical Engineering is a record of the candidates own work carried out by them under my supervision. The matter embodied in this report is original and has not been submitted for the award of any other degree.

Project Supervisor: **Engr. Waqas Javid**

Signature:

Date:

Chairperson (Mechanical): **Dr. Muhammad Yasir**

Signature:

Date:

DEDICATION

We dedicate this project to our families, whose unwavering support and love have been the driving force behind our pursuit of knowledge and academic achievements. Their belief in our abilities and sacrifices made on our behalf have been the pillars of strength throughout our educational journey.

This project is also dedicated to the future generations of aspiring students, researchers, and innovators. May our work serve as an inspiration and contribute to the advancement of knowledge in our field, paving the way for new discoveries and breakthroughs.

May this project be a testament to the collective efforts, determination, and passion of all those involved, and may it leave a lasting impact on our academic and professional journeys.

ACKNOWLEDGEMENT

We would like to express our heartfelt gratitude to **Engr. Waqas Javid**, our dedicated supervisor, for his invaluable guidance, support, and encouragement throughout the development of our Final Year Project Report. His vast knowledge, expertise, and commitment to our success have been instrumental in shaping our project and ensuring its completion.

We extend our deepest appreciation to **Col. Hafiz Sibghat Ullah Fazil (R)** for his valuable insights and assistance in this report. His extensive experience and expertise have significantly enriched our understanding of the subject matter and added depth to our work.

We would also like to thank all the faculty members of our department for their continuous encouragement and for providing us with the necessary resources to carry out this project successfully.

Lastly, we express our sincere gratitude to our friends and colleagues who have supported us throughout the project. Their encouragement, feedback, and collaboration have been invaluable in shaping our ideas and refining our work.

We are indebted to all those mentioned above for their contributions, and we acknowledge their invaluable role in the successful completion of our Final Year Project Report.

ABSTRACT

The report presents a comprehensive study on the mathematical modeling, 3D design, computational fluid dynamics (CFD) simulation, and development of an Unmanned Aerial Vehicle (UAV). The objective of this research was to create a sophisticated UAV design that maximizes performance, stability, and efficiency through the integration of mathematical modeling techniques, advanced 3D design software, and CFD simulations. Based on the findings from mathematical modeling, 3D design, and CFD simulations, a functional prototype of the UAV was developed. The prototype incorporated the optimized design features and components identified through the research process. Flight tests were conducted to validate the performance and stability of the UAV, comparing the results with the predictions from the mathematical models and simulations. The results of this research demonstrate the effectiveness of employing mathematical modeling, 3D design, and CFD simulations in the development of UAVs. The integrated approach enables engineers to optimize UAV designs for enhanced aerodynamic performance, stability, and efficiency. The findings from this study can be used as a foundation for further advancements in UAV technology, contributing to the development of more capable and reliable unmanned aerial systems.

Contents

Table of Figures

1 Introduction

1.1 Historical Background

This section explores the evolution of flying machines, starting with the ancient practice of kite flying and leading to the development of advanced and versatile aircraft, eventually culminating in the concept of quadcopters and feature-rich drones. Kite flying originated approximately 2000 years ago in China, where individuals would fly kites using strings, thereby pioneering the notion of remotely controlled airborne vehicles (RCV). This concept gained popularity worldwide and underwent significant advancements, with China and Japan being instrumental in introducing kites capable of carrying human passengers.

Leonardo da Vinci introduced numerous sketches featuring flying machines and configurations, although they were never put into practice. However, a significant breakthrough occurred in the eighteenth century with the discovery of lightweight hydrogen gas, which yielded fruitful outcomes in the realm of aviation. This led to the introduction of hydrogen gas balloons, marking a milestone in manned flight. France capitalized on this invention and established a balloon company, utilizing these balloons for technical and military purposes. Concurrently, the concept of the bamboo-copter emerged, enabling vertical flights. Additionally, the invention of hot air balloons, based on principles of physics, resolved navigation challenges. During the mid-eighteenth century, the Montgolfier brothers dedicated themselves to aviation experiments, conducting trials with parachutes and balloons in France. Initially employing paper, they later found it unsuitable as the gas caused condensation. Consequently, the concept was refined using electric smoke. Eventually, the French company collaborated with the Montgolfier brothers, harnessing the potential of hydrogen gas and further advancing their ideas. Remarkable achievements were made in the aviation industry, primarily through the lifting effect of balloons capable of carrying human passengers. Thus, the era of manned hot air balloons was ushered in.

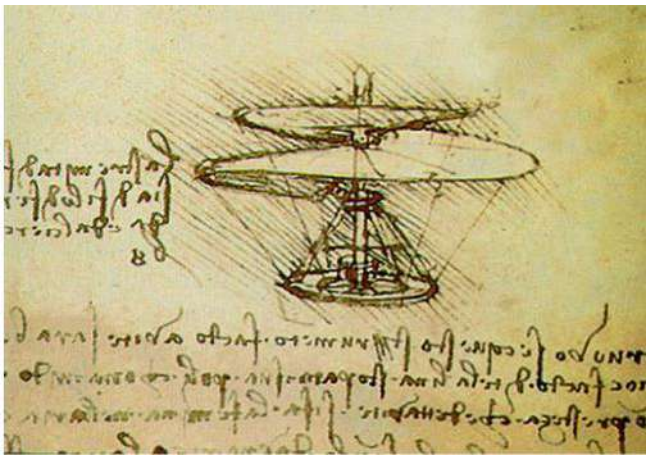

Figure 1 Da Vinci Concept

In the late eighteenth century, Europe embarked on significant developments to address the challenges encountered during balloon and parachute flights. These endeavors focused on understanding the relationship between atmospheric conditions and crucial aviation parameters such as altitude. Tethered balloons found utility in military applications during this time. Additionally, the concept of elongated dirigible balloons emerged, leading to the achievement of the first powered, stabilized, and controlled flight in 1852. This pioneering flight employed a steam engine as its power source, which drove a three-bladed propeller. Another significant advancement occurred in 1884 when collaboration with a French airship company resulted in the first fully stabilized and controllable free flight, following a predetermined path. However, the existing framework was non-rigid, necessitating further advancements in this area.

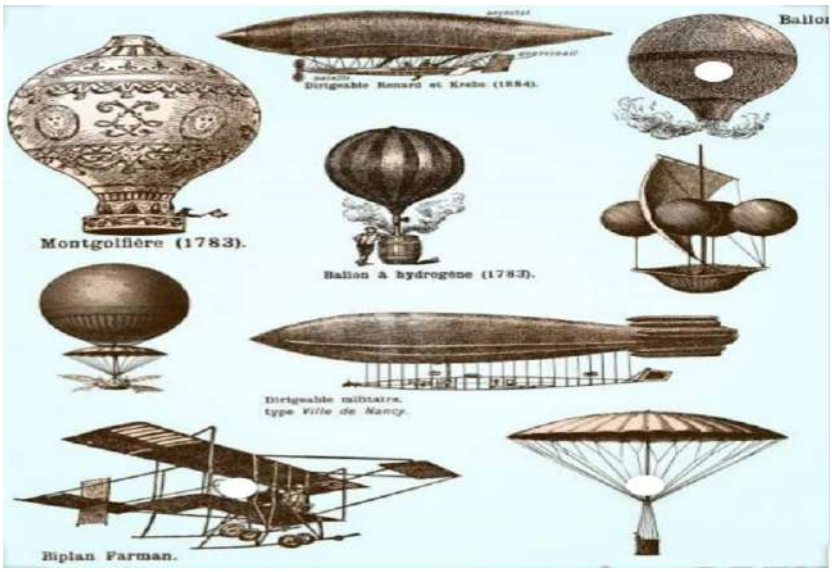

Figure 2: Concept of Elongated Dirigibles and Controlled Flight

Subsequently, the concept of parachutes gained traction and proved to be successful. It became evident that human power alone was insufficient for rigid designs and sustained flights, echoing the predictions of Leonardo da Vinci. Recognizing this need, Robert Hooke devised an ornithopter model fueled by spring forces, which demonstrated the capability of flight. This marked the commencement of endeavors to create truly advanced flying machines, typically incorporating a gondola supported by its canopy and utilizing spring-powered flapping mechanisms for propulsion. These developments led to the introduction of designs for "machines for flying in air," spurring numerous attempts to bring these ideas to fruition.

Sir George Cayley conducted extensive research on the principles of flight and is credited with developing the first modern heavier-than-air aircraft. His studies encompassed a wide range of scientific aerodynamic experiments, leading to the establishment of fundamental principles and the definition of modern aircraft configurations. He even constructed a model helicopter based on the concepts he introduced. In 1799, he outlined the concept of a contemporary aircraft as a fixed-wing flying machine with distinct systems for lift creation, propulsion, and control. His aircraft designs incorporated innovative features, such as a cambered wing instead of a symmetrical one, a separate tail with a horizontal tail plane and fin, and a vertically configured fuselage suspended beneath the center of gravity to ensure stability. Additionally, the design included paddle-like structures, which the pilot could control to function as flap valves. Sir George Cayley also built the world's first full-sized glider. However, his focus primarily remained on gliders and their characteristics, and he did not succeed in creating a fully functional powered aircraft during that time.

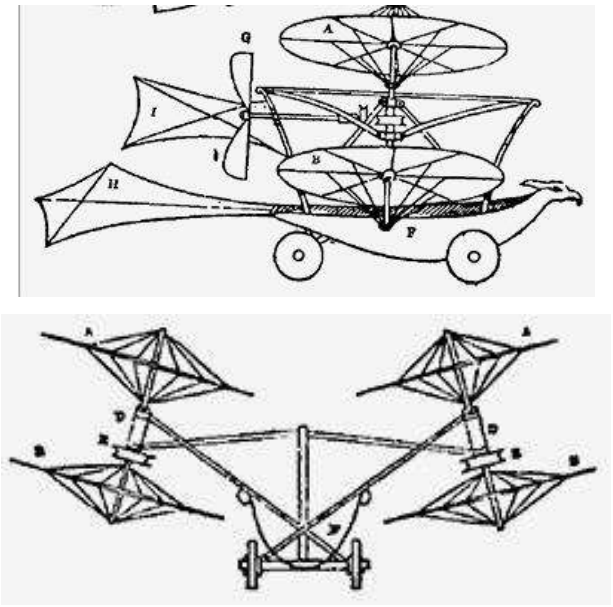

Figure 3 Concept by Sir George Cayley

In 1842, Henson made significant advancements to his design of the aerial steam carriage. His proposal included an aircraft with expansive wingspan, equipped with a steam engine that powered the propellers. The Royal Aeronautical Society conducted extensive research in this field, leading to valuable insights into wing airfoil area and the distribution of lift forces. The invention of the wind tunnel in 1871 further enhanced understanding by revealing the distinctive characteristics of airplanes and offering modified concepts to improve efficiency. During this period, lightweight steam engines were also invented, providing aircraft with the necessary power for flight. Between 1891 and 1896, a series of gliders with various configurations were constructed, marking significant progress and the emergence of practical gliders.

The Wright brothers' contributions to aviation were groundbreaking as they successfully tackled fundamental challenges in flight control and addressed issues that had perplexed earlier aviation pioneers. They conducted meticulous wind tunnel experiments, testing various wing sections, and carried out flying tests with full-sized gliders. Notably, they not only invented a functional powered aircraft but also revolutionized the field of aeronautical engineering. They introduced new instruments and devices into the wind tunnel, enabling the study of drag and lift factors relevant to aircraft. The Wright brothers achieved a significant milestone by creating the first controllable heavier-than-air flying machine that could effectively manage pitch, roll, and yaw movements. Additionally, recognizing the need for sufficient power, they

made notable advancements in the development of internal combustion engines, providing the necessary propulsion for flight. Their innovations and accomplishments propelled the field of aviation forward.

Wright's were able to make first controlled, powered, sustained and heavier-than-air aircraft.

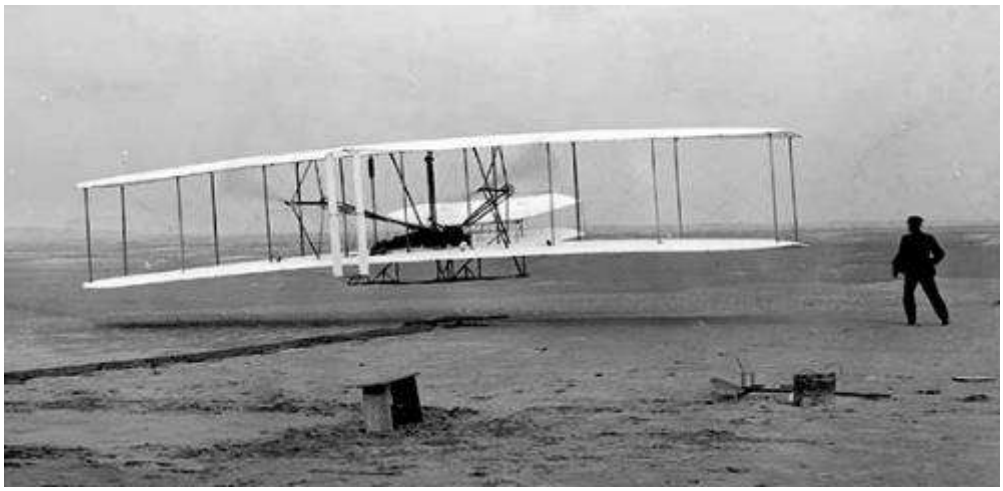

Figure 4Prototype Fixed Wing Airplane Wright Brothers

The period leading up to World War I is often regarded as the pioneering era of aviation, characterized by significant advancements in heavier-than-air aircraft. Innovations in engine design, such as horizontally opposed configurations, brought about revolutionary changes in the aviation industry. These developments resulted in increased lift, improved efficiency, and enhanced stability and control. Subsequent research efforts by aviation pioneers further propelled the field. In 1910, a fully-fledged stable aircraft was introduced, marking a significant milestone.

By 1911, these aircraft were utilized for military purposes, with a British military officer flying an aircraft on a reconnaissance mission. Between 1911 and 1912, operational use of aircraft became more widespread. One notable achievement during this time was the introduction of the "Sikorsky Ilya Muromets," the first four-engine aircraft produced. In 1913, the first prototype of this aircraft took flight, serving both as a bomber and a transport aircraft, showcasing its versatile capabilities.

1.2 What are UAV's

One extension of the acronym UAV is Unmanned Autonomous Vehicle. Autonomous means self-governing, intelligent or independent in taking decisions. With the advent of artificial intelligence in 1980s and 1990s scientists started to carry out research to make technology automated. This implies that machines can be made smart and act like humans. They can sense changes in their surroundings and respond in a predetermined manner. Similarly, efforts are also being made to make UAVS autonomous and "smart" which means that they will be able to take decisions during flight.

UAVs are categorized into following types and details are shown in figure 5 :

- Micro UAVs: small, portable units
- Low altitude, long endurance UAVs
- High altitude, long endurance UAVs employing a conventional design
- High altitude, long endurance UAVs using a low observable design

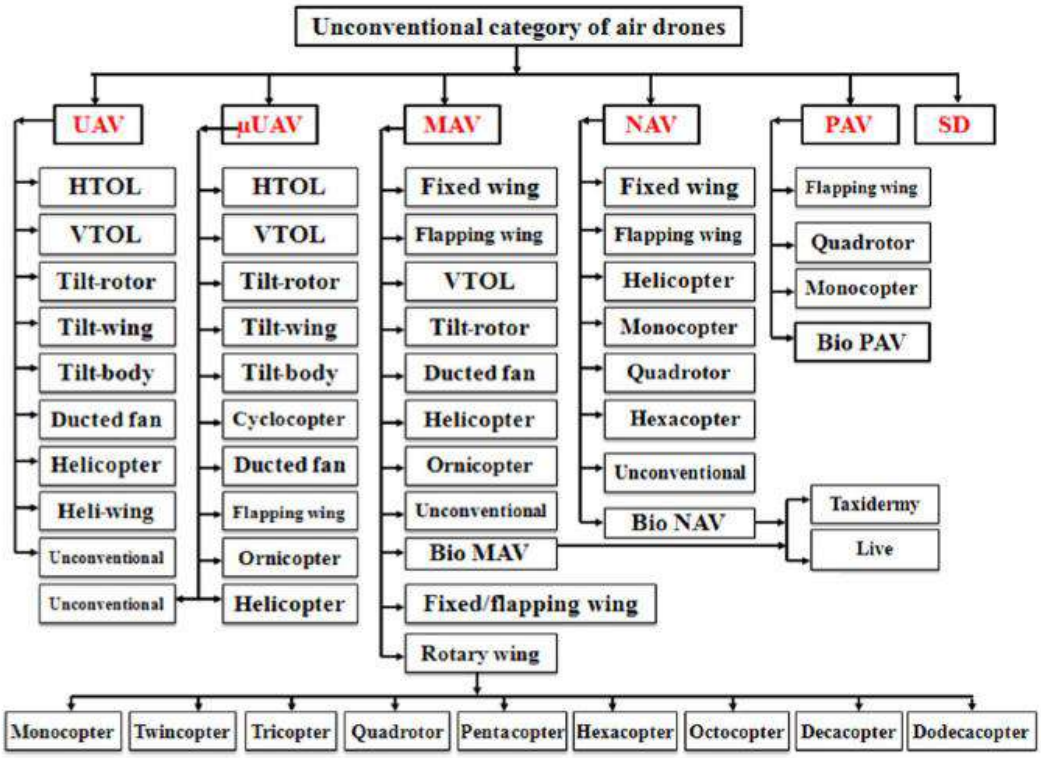

Figure 5: Classification of Drones

1.3 Project Aims and Objectives

The aim of this project is to test fly an electrically propelled remotely controlled UAV with onboard video recording. In order to achieve this aim the following objectives have been determined:

a) Design (Theoretical)
   - ✓ Reference selection
   - ✓ Selection of Airfoil
   - ✓ Lift, Drag, Propulsion etc calculation
   - ✓ Weight Distribution
   - ✓ Performance Calculation
     i. Range
     ii. V_{stall}
     iii. Rate of Climb
     iv. Takeoff Distance
     v. Landing Distance

b) Detailed Design and 3D Modeling (Assembly wit Part Wise Design)
   - ✓ Part Wise Design
   - ✓ Assembly
   - ✓ Final Bill of Quantity (including standard parts)
   - ✓ Engineering Drawings for Manufacturing (Complete Package)

c) CFD Analysis
   - ✓ Meshing
   - ✓ Boundary conditions
   - ✓ Coefficient of Lift and Drag
   - ✓ Pressure Distribution

d) Report
   - ✓ Introduction
   - ✓ Performance Parameters
   - ✓ UAV Specifications
   - ✓ Features
   - ✓ 3D Views

- ✓ Engineering Drawings

1.4 Design Requirement

Following are the design requirement:-

S #	Parameters	Description	British System	SI System
(a)	Aircraft Type	Reconnaissance	-	-
(b)	Weight	Max Takeoff	11.023 lbs	5.0 kg
(c)	Propulsion System	Electric Motor & Prop	-	-
(d)	Endurance	-	15 min	-
(e)	Operational Speed	36km/hr	32.8 ft/s	10 m/s
(f)	Altitude	Operational / Cruise	656.17 ft	200 m
(g)	Range	1 km	3280.8 ft	1000 m
(h)	Payload	Camera / Msc	2.2 lbs	1.0 kg

2 Preliminary Design

2.1 Design Process

A figurative description is shown below:

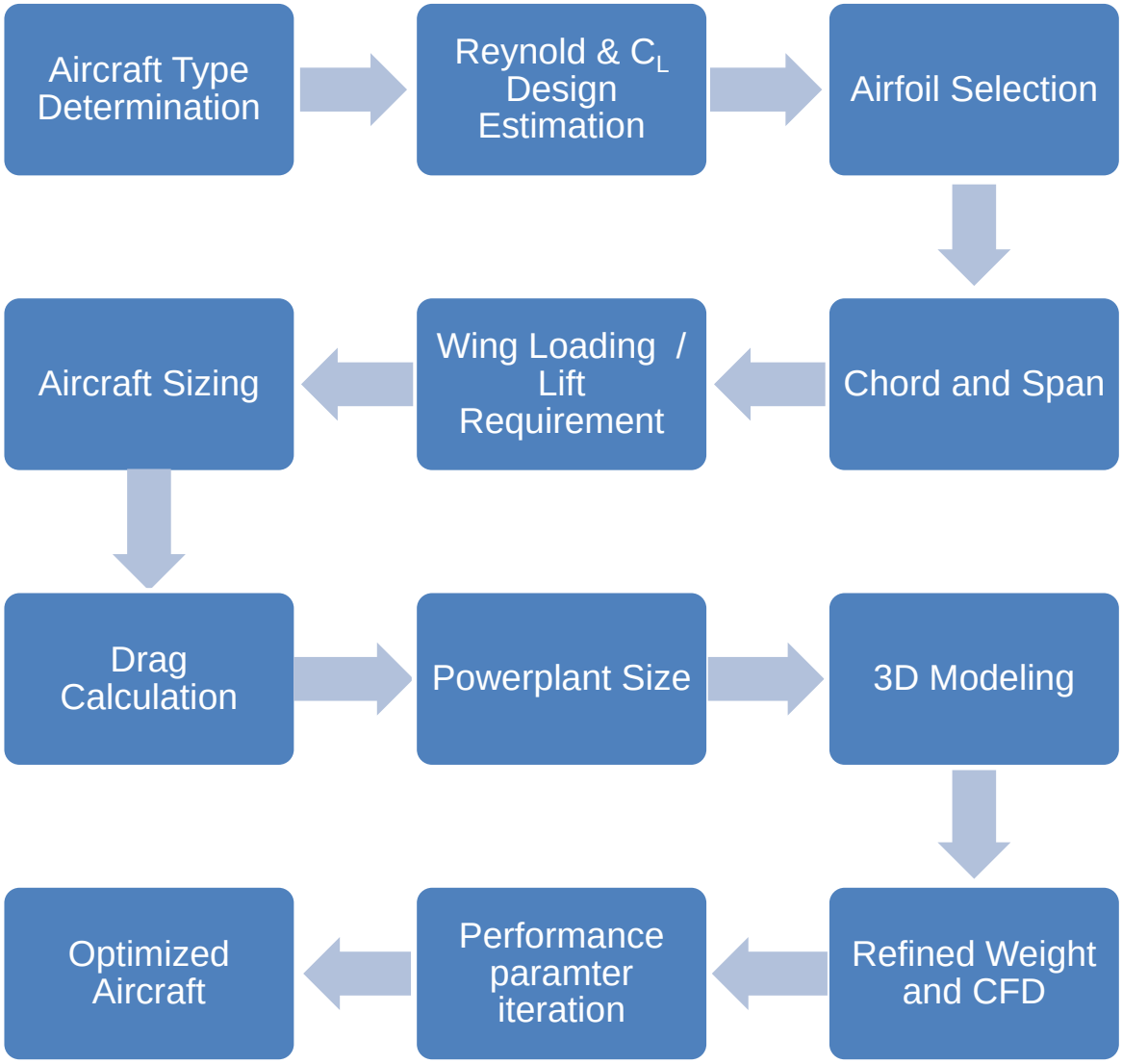

Figure 6: Flow Chart of Design Methodology

2.2 Mission Profile

The mission profile has been split into following major segments which a tactical UAV can foresee / undergo during its life.

(a) Cargo UAV having following mission requirement

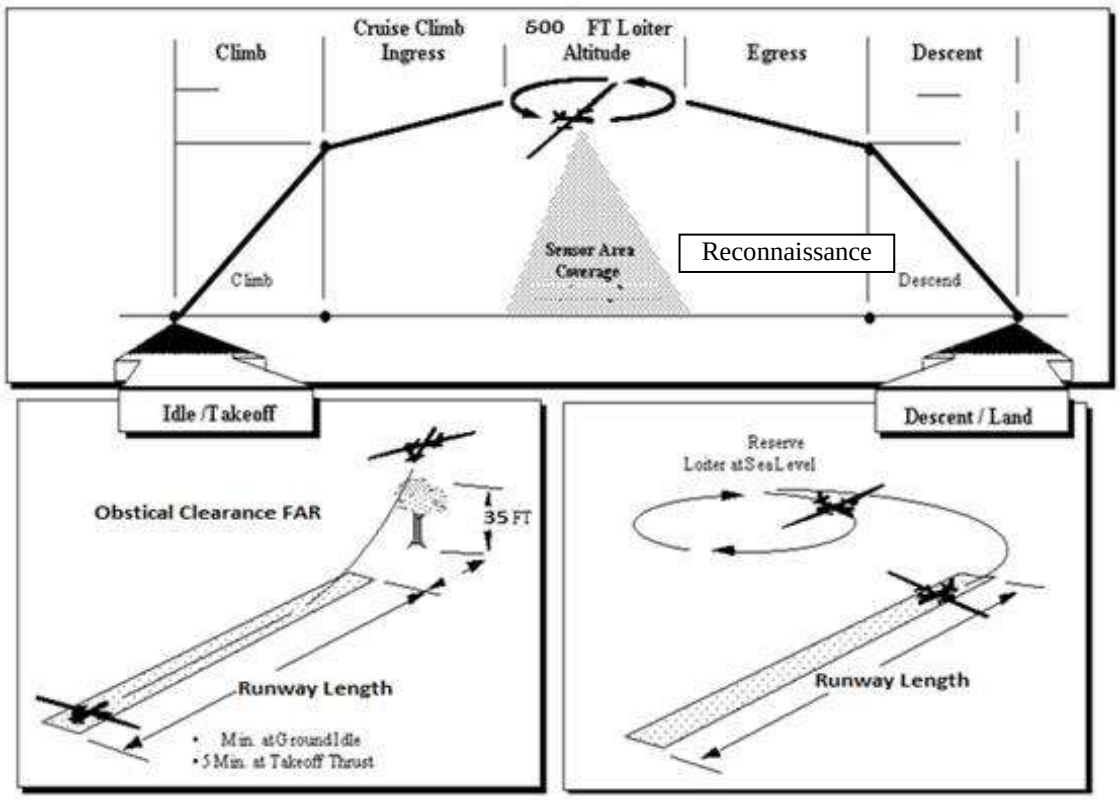

.

Figure 7**:** Mission Profile

S. #	Mission Segment	Remarks
1	Takeoff	Checklist before takeoff approx 2 minutes for manual RC takeoff
2	Climb / Loiter	Climb towards desired altitude say 600ft / 200 meters
3	Cruise Climb	Engaging UAV to area of concern
4	Loiter	Recon over the area
5	Egress	After delivery of package initiating return back
6	Descend	Descend to set altitude

7	Land Loiter	Alignment to runway for landing
8	Land	Safe landing

2.3 Design C_L

C_L design helps us to choose the airfoil which will at least fulfill our requirement to lift the weight. For our safety margin, the preliminary weight is multiplied with 1.5 times and it incorporates all the losses due to the 3D effect or any ideal conditions taken during the design. C_L design will be taken at the cruise speed.

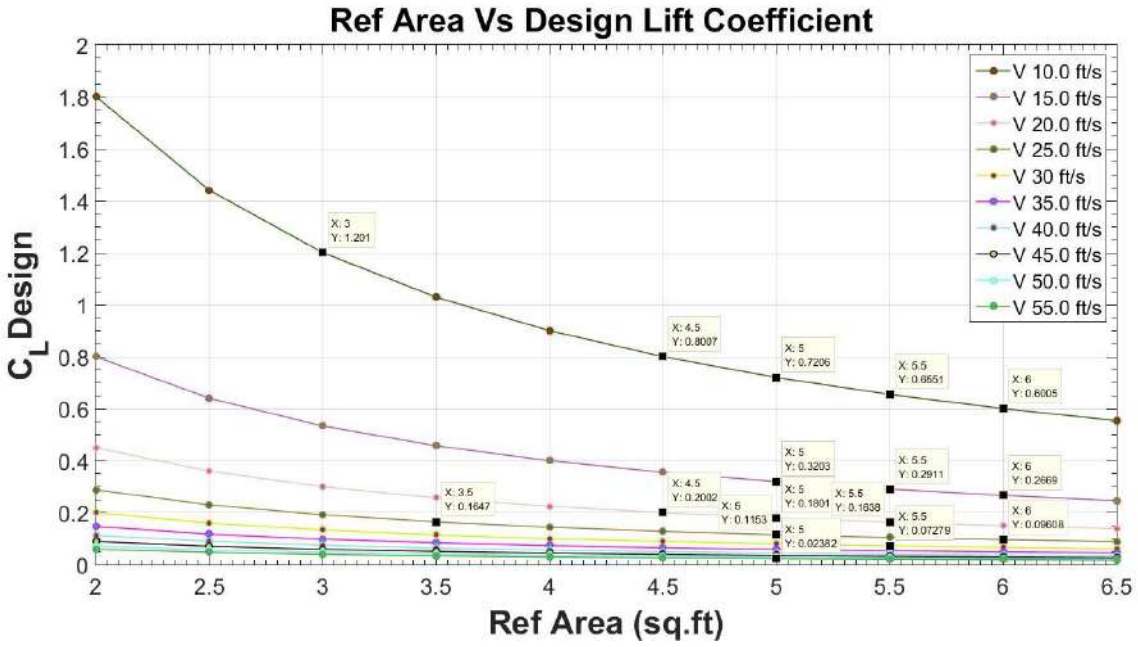

Figure 8: Design Lift Coefficient variation with the reference area at different Velocities

$$\text{Design Lift} = \text{Weight} = C_L \text{ design} \times \frac{1}{2} \times \rho \times V \times V \times S$$

$$C_L \text{ design} = \frac{W}{q \times S}$$

Where 'W' is the weight = 5kg =11.02 lbs x safety factor (1.25) = 13.775 lbs

q Is the dynamic pressure

S is the wing lifting surface area = 5sq.ft

Velocity cruise = V = 15ft/s

$$C_L \text{ design} = \frac{13.781}{2 \times 0.0765 \times 15^2 \times 5}$$

$$C_L \text{ design} = 0.3202$$

2.4 Geometry of Airfoil

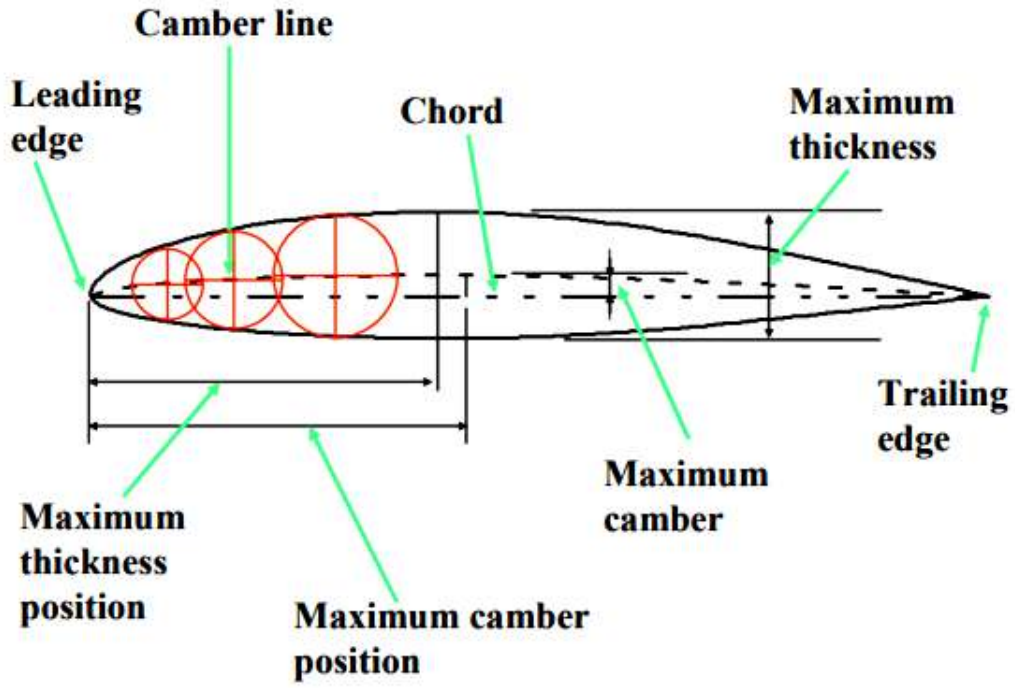

Figure 9: Geometry of Airfoil

Leading edge: The part of the wing that first contacts the air - the foremost edge of an aerofoil.

Chamber Line: The mean camber line is an imaginary line which lies halfway between the upper surface and lower surface of the airfoil and intersects the chord line at the leading and trailing edges.

Chord: It is an imaginary straight line joining the leading edge and trailing edge of an aerofoil. The chord length is the distance between the trailing edge and the point where the chord intersects the leading edge.

Trailing edge: The trailing edge of an aerodynamic surface such as a wing is its rear edge, where the airflow separated by the leading edge meets.

Maximum thickness position: Selected NACA 4412 airfoil section is a 12% thick airfoil which has a 4% maximum camber located at 4/10ths (40%) of the chord.

Chamber Position: The upper surface of the aerofoil will always have a positive camber while the lower surface may have a positive (convex), zero (flat) or negative (concave) camber as appropriate for the intended use.

2.5 Airfoil Selection

The airfoil, in many respects, is the heart of the airplane. The airfoils affects the cruise speed, takeoff and landing distances, stall speed, handling qualities and overall aerodynamic efficiency during all phases of flight.

Following are shortlisted amongst many different airfoils:-

1. S1223
2. E432
3. NACA 4412

Amongst them, only one was to be chosen. Their analysis was done on profili.

2.5.1 S1223

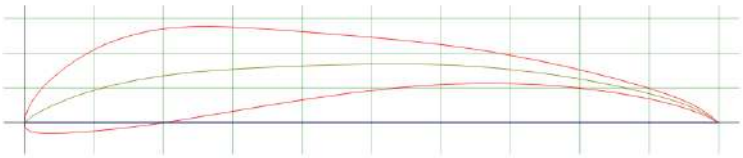

Figure 10: S122

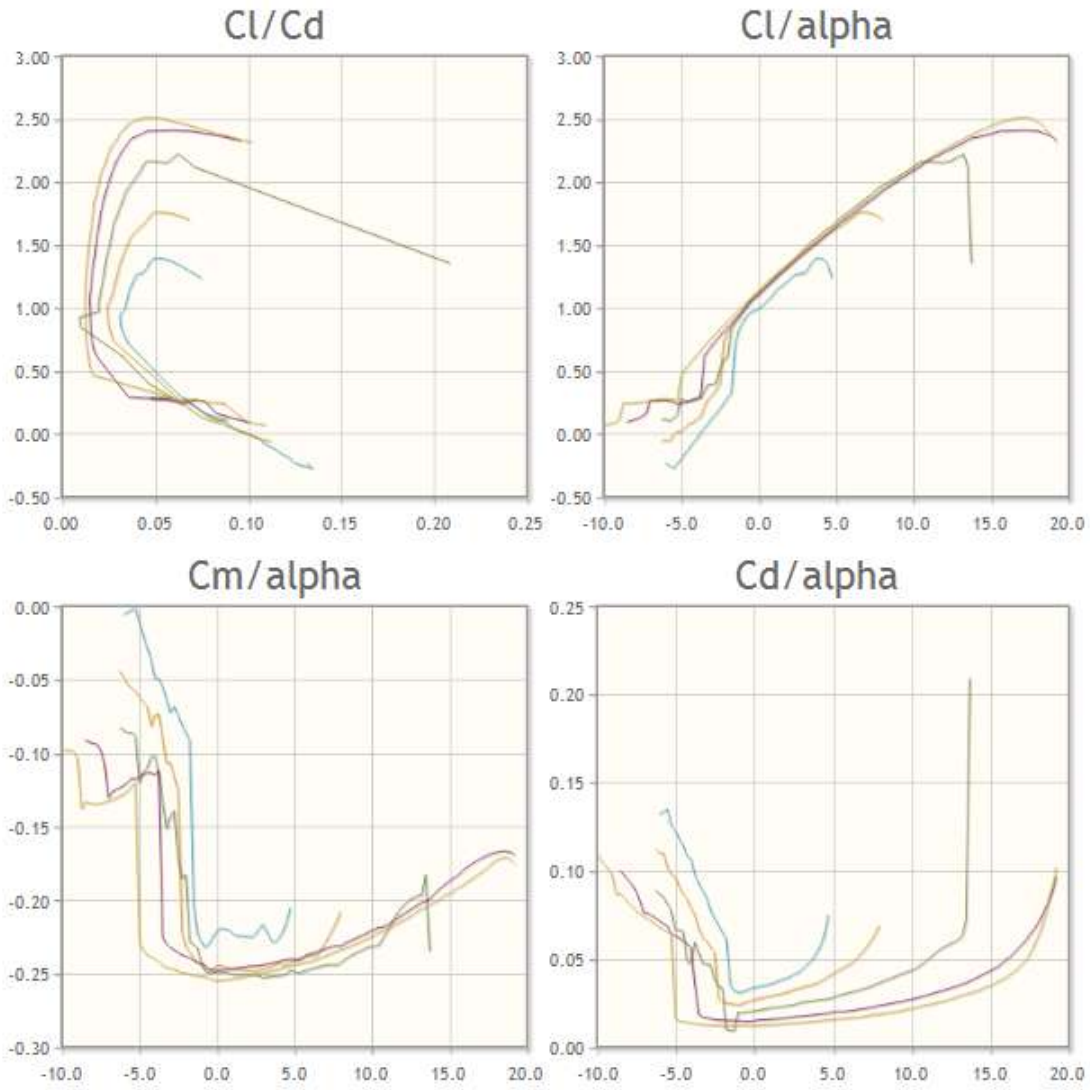

Figure 11: Analysis of S1223

2.5.2 Eppler E432

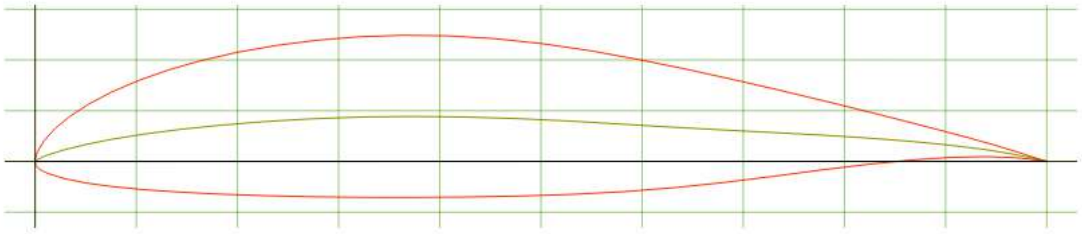

Figure 12: Eppler E432

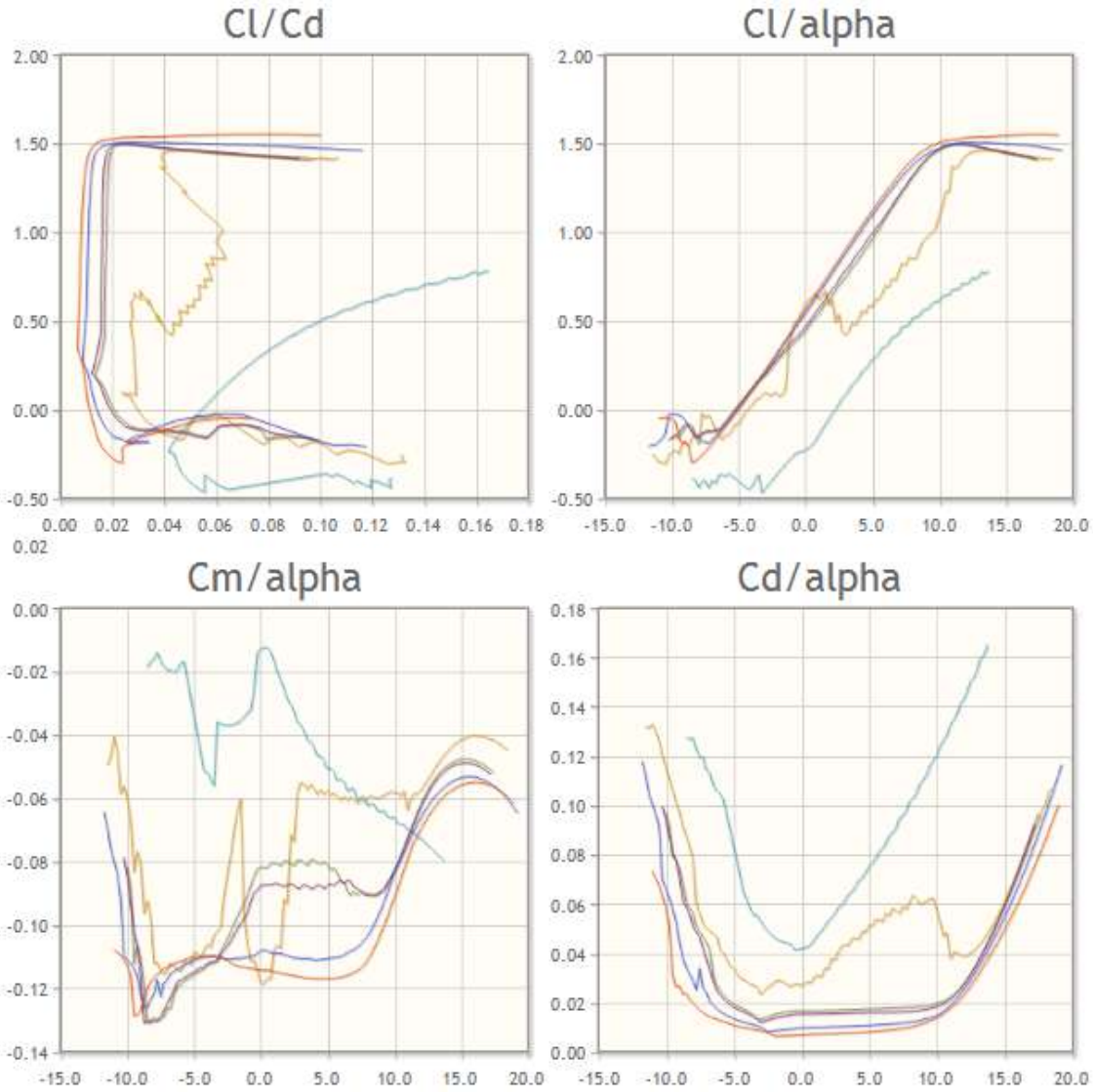

Figure 13: Analysis of E432

2.5.3 NACA 4412

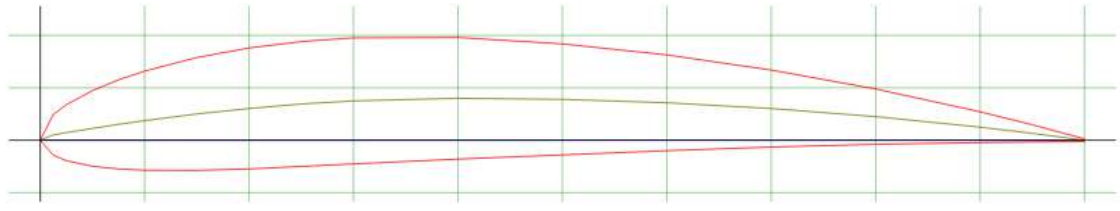

Figure 14: NACA 4412

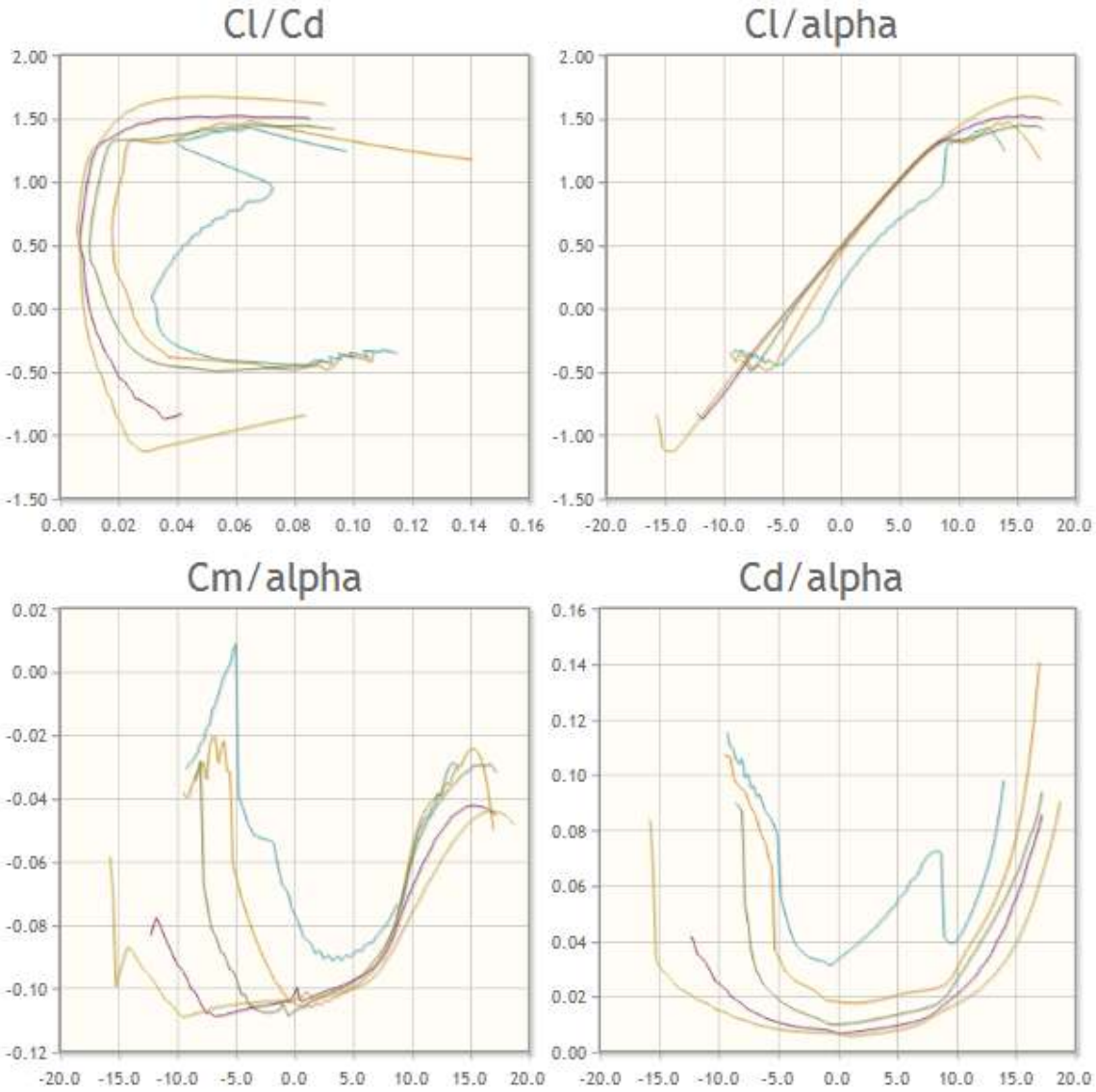

Figure 15: Analysis of NACA 4412

From the analysis of the airfoils, a table of pros and cons was established to determine the airfoil we would need for our aircraft. For manufacturability, the thickness of the airfoil was an important factor. Besides that, a high lift coefficient was preferred for a short takeoff.

Airfoil type	Pros	Cons
S1223	- High Lift. - Comparatively Thin. - Very High L/D Ratio	- Difficult to manufacture. - High pitching Moments which in turn increase tail area to counteract these moments which in turn increases weight. - Comparatively higher drag. - Steep stall
E432	- Low Drag - Moderate Pitching Moments - Easier to Construct - Good L/D ratio	- Lift less as compared to the other 2 airfoils. - Stalls at a lower α. - Thick Airfoil, Increase overall weight.
NACA 4412	- Good, High Lift - Easy to Build - Moderate Thickness - Slow, Steady Stall - Low Drag - Low Pitching Moments - Stalls at a higher α than E432 - Good L/D Ratio	- Cl_{max} lesser than S1223.

Table 1: Selected Airfoils Pros and Cons

From the table, it can be easily seen that we chose NACA 4412 as our airfoil.

2.6 Number of Wings

One of the decisions a designer must make is to select the number of wings. The options are:

1. Monoplane (i.e. one wing)
2. Two wings (i.e. biplane)
3. Three wings

Having more than three wings on an aircraft is generally impractical. The accompanying diagram presents a front view of three aircraft with different configurations. Historically, the primary reason for selecting multiple wings was the limitations of manufacturing technology. A single wing typically required a longer wingspan compared to two wings with the same total area. However, older manufacturing techniques were unable to adequately support a long wing, resulting in instability and lack of rigidity.

Advancements in manufacturing technology, along with the availability of new aerospace materials like advanced lightweight aluminum and composite materials, have rendered this limitation obsolete. As a result, a single wing has become the most practical choice for conventional modern aircraft. In the case of my UAV, I have opted for a monoplane configuration.

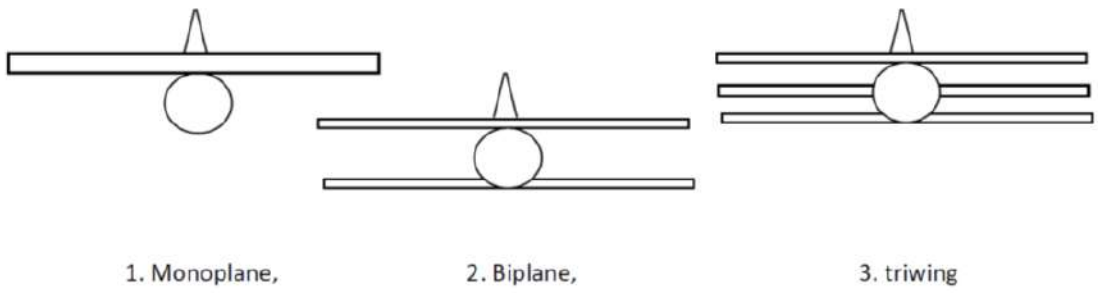

Figure 16 Wing configurations

2.6.1 Monoplane

Advancement in the technology has been made to design a single wing with large dimensions span and considerable stiffness and produced enough lift.

2.6.2 Biplane

- Were used in aerobatic aircraft in era(1960-1980)
- Two wing produce enough lift and reduces turning radius of aircraft
- Disadvantage is the strut and attaches used to hold the wings increases the drag

2.6.3 Tri-plane

- Very rarely used
- Experimental basis, some people tried in the history
- Drag considerably large
- Manufacturing complexities involved

2.6.4 Selected no of wings

- Monoplane Configuration selected
- Lift requirement will be easily met

2.7 Wing Vertical Location

One of the wing parameters that could be determined at the early stages of wing design process is the wing vertical location relative to the fuselage centerline. This wing parameter will directly influence the design of other aircraft components including aircraft tail design, landing gear design, and center of gravity. In principle, there are three options for the vertical location of the wing. They are:

- High wing
- Mid wing
- Low wing

Three of the most common configurations were studied and selection done considering

- Mach no regimes
- Aircraft type

- Stability
- Aerodynamics
- Manufacturing/Mounting complexities

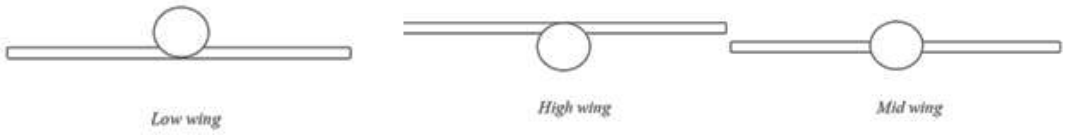

Figure 17 Wing Vertical Location

In general, cargo aircraft have high wing; and most passenger aircraft have low wing. On the other hand, most fighter airplanes have mid wing; while hang gliders and most amphibian aircraft have parasol wing.

The choice of high, mid or low wing configuration depends on the operational considerations associated with the mission of airplane. Effects of wing location on different parameters are described below

2.7.1 High Wing

- Usually homebuilt, aerobatic and low subsonic aircrafts have high wing configurations
- Cargo Aircraft and freight carriers especially military cargo aircraft have high wing configurations
- Turbo-Prop engines mounted on the wing are of high wing configuration to provide ground clearance for the propellers
- Cross wing landing cause the roll moment, and high wing are more safe have enough distance from the ground if the bank angle is increased while landing
- UAV's mostly reconnaissance and packable have the high wing configuration

2.7.2 Mid Wing Configurations

- A compromise between high wing and low wing
- Usually fighters and ground attack aircraft carry bombs and fuel tanks under their wings
- Structural carry through (wing Attachment) is the main problem with mid wings

- Fighters with inlet ducts at the side of fuselage mostly have mid wing configuration
- Mostly UCAV and MALE UAV's have mid wing configurations
- Due to the cabin separation in the passenger aircraft the mid wing is not used in the passenger aircrafts

2.7.3 Low Wing

- Commercial Aircrafts have large dihedrals to increase lift and stability. Thus, the flex due to lift is considerably large and low wing configuration is used.
- Fuel tanks in the wing of commercial aircrafts need safety. Thus luggage apartment is in-between passenger apartment and fuel tanks.
- Wing Box provides enough stiffness for large wings
- The trailing edge flaps near the fuselage and extending down fuselage can be used thus full filling the dihedral lack
- Landing gear stowage and placement in the wing box
- For loading and unloading special carriages and equipment used
- For propeller driven aircrafts with low wing configuration the engine is mounted above causes the interference drag and effects between propeller and wing

2.7.4 Selected wing Vertical Location

- UAV low subsonic
- Ground visibility when camera mounted
- Much stability required because gross weight is too small and gust will be largely effecting the spiral and roll stability
- Increase lift
- Easily mounted on the fuselage if UAV is packable

Factor	**High Wing**	**Mid Wing**	**Low Wing**
Stability	(Points)	(Points)	(Points)
1) Roll	5	4	3
2) Spiral	5	4	3
Maneuverability			

1) Low subsonic	5	4	3
2) Subsonic	4	5	3
3) Supersonic	3	5	4
Dihedral Effect	5	4	3
Landing Gear			
1) Wing Mounted	3	4	5
2) Fuselage Mounted	4	3	5
Visibility	5	4	3
Fuselage interference			
1) UAV's	5	4	3
2) Passenger	4	3	5
3) Fighter	3	5	4
Engine Pod and interference			
1) UAV's	5	4	3
2) Jet Fighter	3	5	4
3) Commercial	3	5	4
4) Propeller	5	4	3

Table 2 Selected wing configuration

The **high wing** configuration was selected because it was at most advantage to use in our UAV.

2.8 Wing Tips

Common Types of wing Tips are studied which are as follows

1. Rounded
2. Sharp Edge
3. Cutoff
4. Hoerner
5. Dropped
6. Unswept
7. Aft-Swept
8. Cutoff Toward swept
9. End Plate

10. Wing let

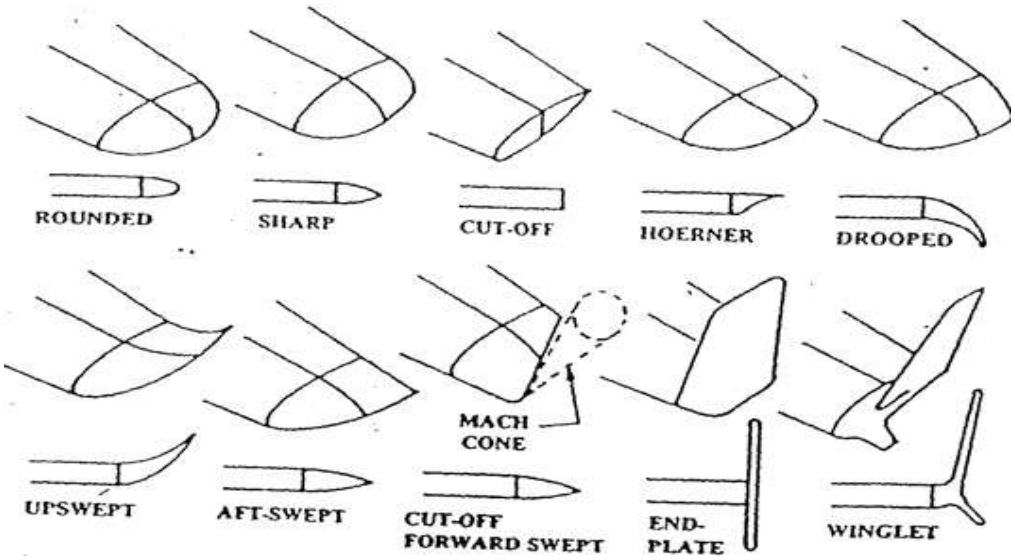

Figure 18 Wing tips

2.8.1 Effect of wing tips

(a) **Rounded:** Aircraft wetted area effect only a small extent. Rounded tips easily permit air to flow around the sharp tips

(b) **Sharp Edge:** Lateral spacing of wing tip vortices

(c) **Cutoff:** Simple cutoff tips have lesser drag than rounded

(d) **Sharp Edge:** Sharp edge also minimizes the drag

(e) **Hoerner:** Hoerner increases the effective span

(f) **Aft-Swept:** Aft Sweep with greater trailing edge reduces drag wing tips vortices appear at trailing edge

(g) **Cutoff Toward swept:** Cut off forward swept used in supersonic aircraft

(h) **End Plate:** End plate wetted area causes the drag

(i) **Wing let**: Wing lets to reduce the energy of wing tip vortices and reducing the drag coefficient but complex to design

2.8.2 Selected wing tips

Cutoff Type

- Wing tips are selected as cut off for reducing the induced drag without having extra weight and complexity.

2.9 Wing Dihedral

Dihedral for a wing could be

1. Dihedral angle at root
2. Tip dihedral
3. Poly-dihedral

It is added to obtain

- Stabilize the torque produced by propeller in specific direction
- Reduces the side slip and increases the lift distribution

- Gust and external disturbance causes the roll and spiral effect, dihedral reduces these effects
- Effective, turning and bank angles
- Excessive dihedral produces the Dutch roll
- Estimated Dihedral for homebuilt and UAV's for good performance are taken 2deg at the root. Initial Estimate taken as

Dihedral at root = **2deg**

2.10 Wing incidence

- Wing incidence angle is ultimately set by using wind tunnel testing results.
- Pitch Angle with respect to fuselage
- To minimize drag at cruise conditions
- Raymer page 52 suggests angle of incidence of 2deg for the homebuilt and low subsonic aircrafts
- We choose 2deg incidence angle because Cl_{design} is 0.3202 and at cruise it is easily achievable at angle of attack 2deg.

2.11 Wing twist

Wing twist is an aerodynamic characteristic incorporated into aircraft wings to adjust the distribution of lift across the wing. Its primary objective is to ensure that the wingtip remains the last part of the wing surface to stall, particularly during maneuvers such as rolls or steep climbs. This is achieved by applying a small downward twist to the wingtip compared to the rest of the wing.

By implementing this twist, the effective angle of attack at the wingtip is consistently lower than at the root, ensuring that the root stalls before the tip. This is advantageous because flight control surfaces are typically situated at the wingtip. The variable stall characteristics of a twisted wing provide an indication to the pilot of an impending stall, while still allowing the control surfaces to remain effective. As a result, the pilot can typically prevent a complete stall before losing full control of the aircraft.

In our initial design, we have chosen a wing twist of 0 degrees, which will provide us with sufficient stall characteristics.

2.12 Leading Edge Wing Sweep:

- Sweep is given to the wing to reduce the adverse effects of transonic and supersonic flow. Sweep have several advantages which include the stability and compensation drag divergence Mach no
- As our UAV is subsonic, so we have selected the leading edge sweep equals to zero

2.13 Tail Geometry and Arrangement:

- Major contribution of lift is by wing
- Tail contributes to the lift but provide trim (to balance extra moments), stability and control
- Vertical tail to generate enough forces in case of engine failure and gusts or coordinated turns
- Vertical tail area to dampen dutch roll and stability

2.13.1 Conventional Tail

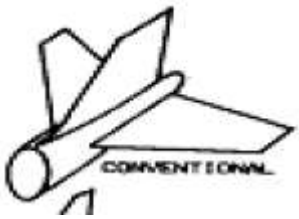

- Large areas
- Vertical tail much effective
- Fuselage interfaces
- Lightest of the weight
- No mounting difficulties
- 70% aircraft in the world have this type of configuration
- Adequate stability and control
- Best for the Conventional type aircraft

2.13.2 T-Tail:

- Inherently heavier than conventional

- Horizontal stabilizer located at the top to prevent wake of an engine mounted as in business jets
- Effective horizontal stabilizer
- Reduced aerodynamic interference
- Flutter difficulties to handle at horizontal stabilizer
- Helpful, effective and Easy to recover in stall

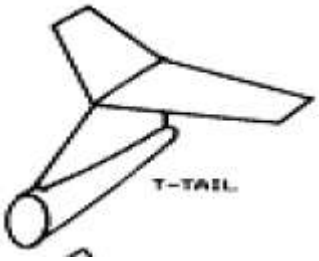

2.13.3 H-Tail

- To avoid propeller wash H-tail is used
- More effective at high angle of attack because no fuselage interference flow
- End plate effect increases the efficiency of the horizontal tail
- Two rudders reduces the area of horizontal tail

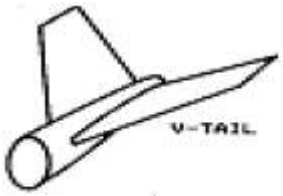

2.13.4 V-Tail

- To reduce the wetted area
- Complex to analyze
- Pythagorous theorem used to find the velocities parameters and then their resultant to give force in the direction for yawing and pitching
- V-tail provides the effective and considerable stability and control
- Reduced wetted area, reduces the interference drag
- Usually span is greater as compared to the horizontal tail

2.13.5 Twin Tail

- Height requirement reduction using h-tail
- More effective
- Modern aircraft especially fighters have this configuration
- Fuselage interference is reduced
- Heavier than other tail configurations

2.13.6 Boom Mounted

- Best for the pusher type propeller configuration

- The downwash and side slip produced by the fuselage is reduced in this configuration
- Two vertical stabilizers reduces the size and increases the effectiveness
- The end plate design also gives the wing tip effect and increases the efficiency of the horizontal tail
- Away from the fuselage interference
- Side to side (Dutch roll) motion is easily tackled

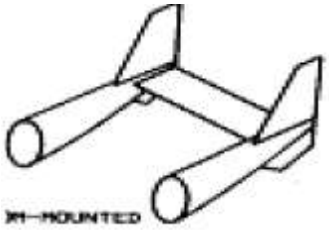

2.13.7 Others Parameters Considered

- Spin recovery
- Dutch roll
- Spiral Stability
- Spin recovery such that rudder effective at high angle of attack and it is provided either by the twin tail or boom mounted tail
- At the high angle of attacks the tail is stalled
- Moreover, the pusher configuration considered for our aircraft thus the horizontal stabilizer to avoid wake must be placed at the top of vertical tail
- Since, our UAV is small and subsonic thus no vertical and dorsal tail is required

Considering the above points we come to conclusion that best tail configuration for our aircraft is **Conventional tail**

2.14 Wing Aspect Ratio

Aspect Ratio can be defined as

$$AR = \frac{b^2}{S}$$

By trying at different span (b) and wing area Area (S) we plotted following graph:-

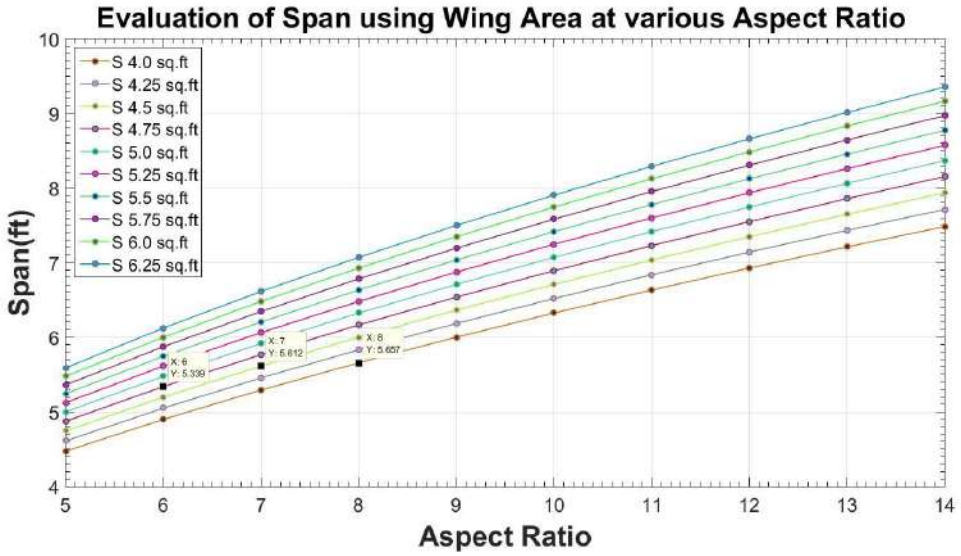

Figure 19: Aspect ratio vs Span

Span selected: 5.612 ft

AR will be 7

2.15Wing geometry

2.15.1 Span:

$$b = \sqrt{AR * S}$$

$$b = \sqrt{7 * 4.5}$$

$$b = 5.612\ ft$$

2.15.2 Root chord:

$$C_{root} = \frac{2S}{b(1+\lambda)}$$

For $\lambda = 1.0$

$$C_{root} = 0.802\ ft$$

2.15.3 Mean Aerodynamic chord

$$\overline{c} = \frac{2}{3} C_{root} \frac{(1 + \lambda + \lambda^2)}{(1 + \lambda)}$$

Putting the values we get,

$$\bar{c} = 0.802 \text{ ft}$$

2.15.4 Location of Mean Aerodynamic Chord from centerline:

$$\overline{Y} = \left(\frac{b}{6}\right)\left[\frac{(1 + 2\lambda)}{(1 + \lambda)}\right]$$

$$\bar{Y} = 1.403 \text{ ft}$$

2.16 Fuselage Sizing

Fuselage length is estimated as from the **following table (Raymer)**

Fuselage length vs W_0

Length $= a W_0^C$	a	C
Sailplane—unpowered	0.86	0.48
Sailplane—powered	0.71	0.48
Homebuilt—metal/wood	3.68	0.23
Homebuilt—composite	3.50	0.23

Table 3 Fuselage length Vs. Wo

Real world fuselage design also depends upon no of factors like

- Crew
- Payload
- Passengers
- Cargo etc.

Here, from the above table the values for constants for Home built composite are taken as

$$Length = aWo^{c}$$

$$Length = 3.50 * 11.02^{0.23}$$

$$Length = 6.08\ ft$$

2.17 Horizontal tail

The tail of an aircraft counters the moments produced by the wing. Tail sizing is estimated using a historical approach for initial design purposes.

Forces due to tail lift are proportional to the tail area. The tail effectiveness is proportional to the tail area times moment arm and is called the tail volume co-efficient

$$\mathrm{CHT} = \frac{\mathrm{L_{ht}} * \mathrm{S_{HT}}}{\mathrm{C_W S_W}}$$

L_{ht} can be taken as 2.5-3 times of the wing chord thus, confirming the distance compatibility

$$\mathrm{L_{ht}} = 2.8 * 0.802$$

$$\mathrm{L_{ht}} = 2.2456\ \mathrm{ft}$$

Taking $\mathrm{L_{ht}} = 2.2456$ ft

$$\mathrm{S_{HT}} = \frac{0.5 * 0.802 * 4.5}{2.2456}$$

$$\mathrm{S_{HT}} = 0.804\ \mathrm{ft^2}$$

Table 4.3 Tail aspect ratio and taper ratio

	Horizontal tail		Vertical tail	
	A	λ	*A*	λ
Fighter	3–4	0.2–0.4	0.6–1.4	0.2–0.4
Sail plane	6–10	0.3–0.5	1.5–2.0	0.4–0.6
Others	3–5	0.3–0.6	1.3–2.0	0.3–0.6
T-Tail	–	–	0.7–1.2	0.6–1.0

Figure 20 Raymer Aircraft Design recommended values

- Horizontal tail aspect ratio 5

- Taper ratio considering 0.4
- Sweep 20 deg

Table 6.4 Tail volume coefficient

	Typical values	
	Horizontal c_{HT}	Vertical c_{VT}
Sailplane	0.50	0.02
Homebuilt	0.50	0.04

Horizontal tail span

$$b = \sqrt{AR * S_{HT}}$$

$$b = \sqrt{5 * 0.804}$$

$$b = 2.004 \text{ ft}$$

2.17.1 Root chord

$$C_{ROOT} = 2 * \frac{S}{[b(1+\lambda)]}$$

$$C_{ROOT} = 2 * \frac{0.804}{[2.236(1+0.4)]}$$

$$C_{root} = 0.572 \text{ ft}$$

2.17.2 Tip chord

$$C_{tip} = \lambda C_{root}$$

$$C_{tip} = 0.4 * 0.572$$

$$C_{tip} = 0.2291 \text{ ft}$$

2.17.3 Mean Aerodynamic chord

$$MAC = \frac{2}{3} * C_{Root} * \frac{1 + \lambda + \lambda^2}{1 + \lambda}$$

$$MAC = \frac{2}{3} * 0.572 * \frac{1 + 0.4 + 0.4^2}{1 + 0.4}$$

$$\text{MAC} = 0.4254 \text{ ft}$$

2.17.4 Location of maximum MAC

$$Y = \frac{b}{6}\left(\frac{1+2\lambda}{1+\lambda}\right)$$

$$Y = \frac{2.004}{6}\left(\frac{1+2*0.4}{1+0.4}\right)$$

$$Y = \frac{2.004}{6}\left(\frac{1.8}{1.4}\right)$$

$$Y = 0.429 \text{ ft}$$

2.18 Vertical Tail:

- Vertical tail aspect ratio 1.2
- And taper ratio 0.9
- Vertical tail sweep angle is taken 35-55deg for the low subsonic aircrafts (Ref: Page no 76, Raymer aircraft design) thus taking 40 deg

2.18.1 Vertical Tail Area

We have

$$S_{VT} = \frac{C_{VT} b_W S_W}{L_{VT}}$$

C_{vt} taken as 0.04

$L_{VT}=L_{HT}$ is taken as the same as before = 2.8 ft

b_w wing span= 5.612 ft

$$S_{vt} = 0.361 \text{ ft}^2$$

2.19 Vertical tail span

$$b = \sqrt{AR * S_{VT}}$$

$$b = \sqrt{1.2 * 0.361}$$

$$b = 0.6579 \text{ ft}$$

2.20 Root chord

$$C_{ROOT}=2*\frac{S}{[b(1+\lambda)]}$$

$$C_{root} = 0.7833 \text{ ft}$$

2.21 Tip chord

$$C_{tip} = \lambda C_{root}$$

$$C_{tip} = 0.313 \text{ ft}$$

2.22 Mean Aerodynamic chord

$$MAC = \frac{2}{3} * C_{Root} * \frac{1 + \lambda + \lambda^2}{1 + \lambda}$$

Putting values we get,

$$MAC = 0.5819 \text{ ft}$$

2.23 Location of maximum MAC

$$Y = \frac{b}{6}\left(\frac{1 + 2\lambda}{1 + \lambda}\right)$$

Plugging in the values we get,

$$Y = 0.1409 \text{ ft}$$

2.24 Control surfaces

Ailerons, rudders and elevators are the primary control surfaces for effecting roll, yaw and pitch respectively.

2.25 Ailerons

- Outboard ailerons are used most often due to their effectiveness
- Frise ailerons which reduces adverse yaw
- For high sweep angles the outband ailerons are not effective since our wing is not swept and subsonic also thus we can use outboard ailerons nor we have to do combat role
- They are extended from 50% to 90% of the wing semi span and chord varies from 15-25%

$$\frac{\text{span of ailerons}}{\text{wing span}}=0.42$$

$$\frac{\text{aileron chord}}{\text{wing chord}} = 0.2$$

These are calculated by the following **figure**

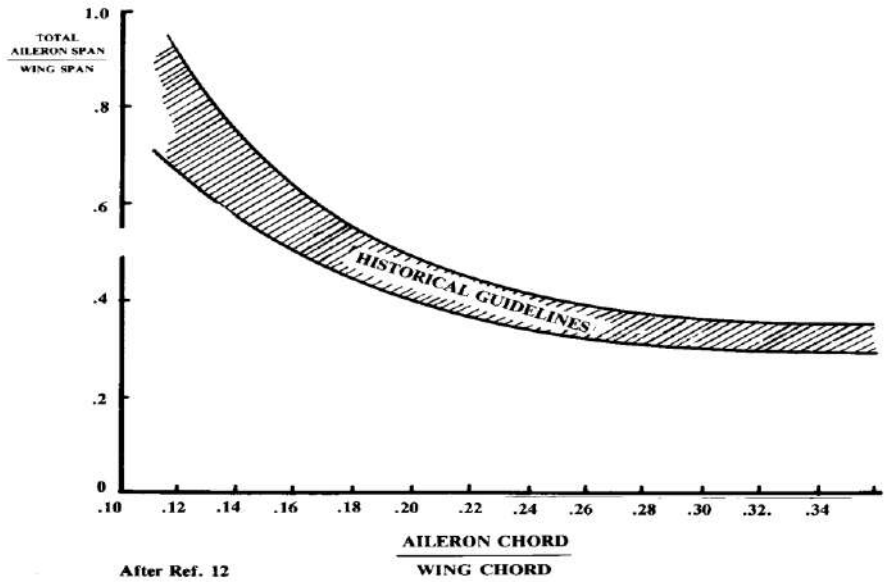

Figure 21

Thus,

$$\text{span} = 0.42 * 5.612$$

$$\text{span} = 2.36 \text{ ft}$$

And,

$$\text{chord} = 0.2 * 0.802$$

$$\text{chord} = 0.1604 \text{ ft}$$

2.26 Elevator

Typically extend to the tip of the tail about 90 %. The span is usually 25-50% of tail chord. Estimation done on historical data as

Span is 90% of horizontal tail span

$$span = 0.9 * 2.004$$

$$span = 1.804\ ft$$

Chord is 30 % of horizontal tailchord MAC

$$chord = 0.3*0.4254$$

$$chord = 0.1276\ ft$$

2.27 Rudders

Rudders again taking the common practices, span is 90% of vertical tail span and chord is 30 % of vertical tail chord MAC

$$\text{span} = 0.9 * 0.65799$$

$$\text{span} = 0.5922 \text{ ft}$$

$$\text{chord} = 0.3 * 0.5819$$

$$\text{chord} = 0.1745\text{ft}$$

2.28 Summary Of All Refined Sized Components

2.28.1 Wing

Table 4 Wing Summary

Airfoil at root and tip	4412 (NACA)
Span	5.612 ft / 1710.54mm
C_{root}	0.802 ft / 244.45mm
C_{tip}	0.802 ft / 244.45mm
MAC(c)	0.802 ft /244.45mm
Y(MAC)	1.403 ft / 427.63mm
Aileron	Outboard
Aileron span	2.3572 ft / 718.47mm
Aileron chord	0.1604 ft / 48.89mm
Wing area (S)	4.5 ft^2
Wing Dihedral Angle	0 deg
Wing Twist	0 deg
Wing Incidence	2 deg
Wing Tip	cutoff
Wing Vertical Location	High wing
Wing Aspect Ratio	7.0
Leading Edge Sweep	0deg
Quarter Chord Sweep	0deg

2.28.2Horizontal tail

Airfoil	Flat Plate
Span	2.004 ft / 610.82mm
Croot	0.572 ft / 174.35mm
Ctip	0.2291 ft / 69.83mm
MAC	0.4254 ft / 129.66mm
Y(MAC)	0.4295 ft / 130.91mm
Elevator span	1.804 ft / 549.86mm
Chord	0.1276 ft / 38.89mm
Lht	2.8ft / 853.44mm

Leading Edge Sweep	20deg

Table 5 Horizontal tail

2.28.3Vertical tail

Area (Svt)	0.3608 ft / 109.97mm
Span (b)	0.658 ft / 200.56mm
Croot	0.7833 ft / 238.75mm
Ctip	0.313 ft / 95.40mm
Rudder span	0.5922 ft / 180.50
Rudder Chord	0.1746 ft / 53.22
MAC	0.5812 ft / 177.15mm
Y(MAC)	0.1409 ft / 42.95mm
Leading Edge Sweep	40deg

Table 6 Vertical tail

2.29 Fuselage

Length	6.078 ft / 1852.57

Table 7 Fuselage

3 Drag Estimation

Total Drag will be equal to the drag contribution of all individual components of an aircraft. The breakdown can be given as follows

$$\text{Airplanedrag} = \text{Componentdragof "(wing} + \text{fuselage} + \text{empennage} + \text{nacelle} + \text{flaps} + \text{landinggears} + \text{canopy} + \text{store} + \text{trim} + \text{interference} + \text{miscellaneous)"}$$

Total Airplane drag is given as

$$D = C_D \bar{q} S$$

And from Roskam drag prediction equation taken from part 6

$$C_D = Cd_{wing} + Cd_{empennage} + Cd_{fuselage} + Cd_{flap} + Cd_{gear} + Cd_{trim} + Cd_{msc} + Cd_{canopy} + Cd_{interference} + Cd_{Nacelle}$$

3.1 Wing Drag Coefficient Prediction:

$$Cd_{wing} = Cd_{ow} + Cd_{LW}$$

Where $Cd_{ow}$the zero wing lift drag coefficient and $Cd_{LW}$is the wing lifting drag coefficient

$$Cd_{ow} = (R_{wf})(R_{ls})(Cf_w)\left(1 + L'\left(\frac{t}{c}\right) + 100\left(\frac{t}{c}\right)^4\right) Swet_{wing}/S$$

R_{wf} is wing to fuselage interference factor, $R_{ls}$is lifting surface correction factor

Cf_w is turbulent flat plate friction coefficient and L' is the Airfoil thickness location parameter

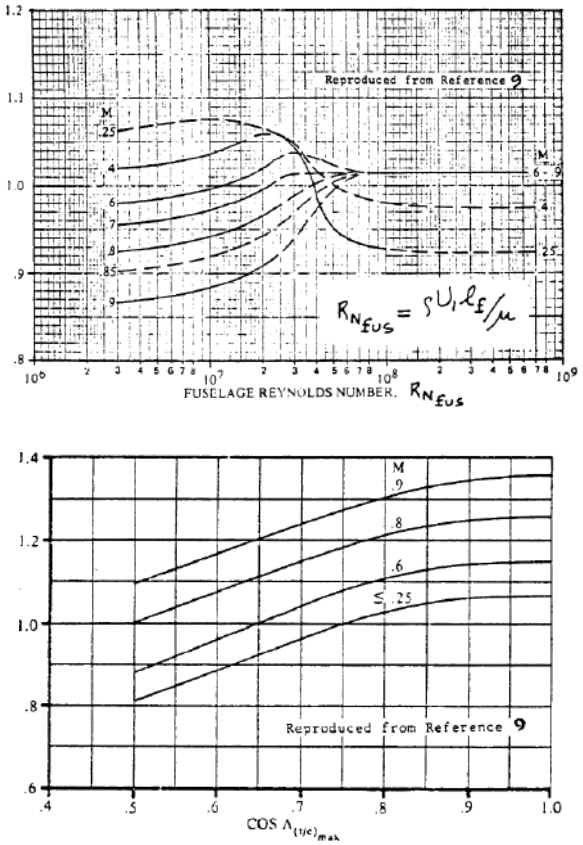

Figure 22 (a) Fuselage Reynolds Number Vs Rwf (b) Rls Reynolds Vs Sweep Angle

$$R_{wf} = 1.08 \; and \; R_{ls} = 1.07$$

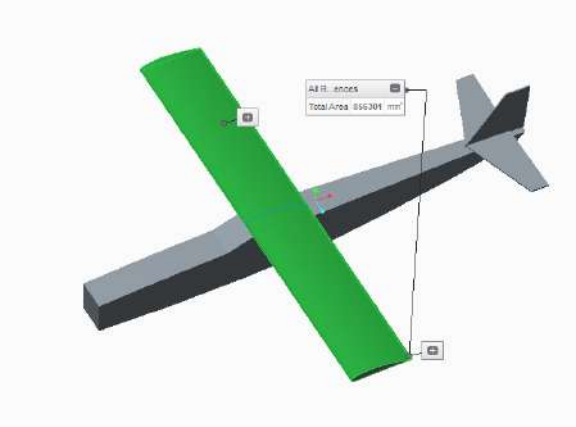

Figure 23 (a) Reynold Number Vs Cf (b) S_{wet} wing

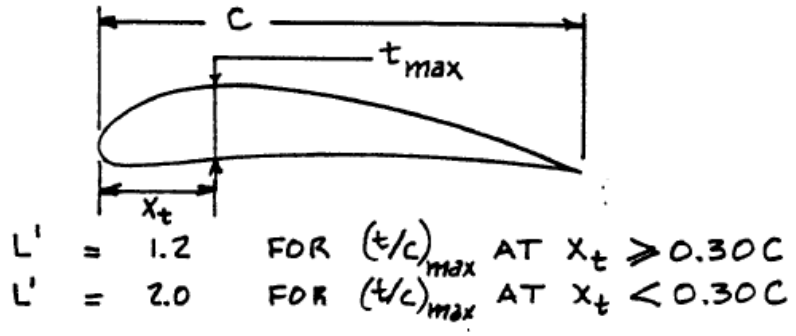

Figure 24: L' selection based on t/c

From figure3.7 above, L' is taken 1.2 for (t/c)max of 0.12 at 30%

3.2 Zero Lift Drag of Wing

S_{wet} already calculated as $Swet_{wing} = 9.217$ ft^2=0.86m^2

$S_{ref} = 4.5$ ft^2=0.42m^2

plugging in all the values for Cd_{ow}we get,

$$Cd_{ow} = (R_{wf})(R_{ls})(Cf_w)\left(1 + L'\left(\frac{t}{c}\right) + 100\left(\frac{t}{c}\right)^4\right)Swet_{wing}/S$$

$$Cd_{ow} = (1.08)(1.07)(0.0043)((1 + 1.2\ (0.12) + 100(0.12)^4)0.86/0.42$$

$$Cd_{ow} = 0.0117$$

Now, wing drag coefficient

$$Cd_{LW} = \frac{Clw^2}{\pi Ae}\ 2\pi.\ Cl_w\varepsilon_t v + 4\pi^2(\varepsilon_t)^2 w$$

Where, e is the (Ostwald's efficiency factor) = 0.7875, ε_t is the wing twist angle (zero), v is the induced drag factor due to linear twist and w is zero lift drag factor due to linear twist Cl_w is the wing coefficient and defined as

$$\mathrm{Clw} = \mathrm{Cl} - \frac{\mathrm{Cl_C S_C}}{\mathrm{S}} + \mathrm{Cl_h S_h}$$

Where,

$\mathrm{Cl_C}$ is canard lift coefficient zero in our case, Cl_h is horizontal lift coefficient determined from trim considerations, thus ignoring at this stage. C_{lw} is found out using design Cl or weight and area used in simple lift equation. Both are close enough

$$\text{Cl-w} = \frac{\mathrm{W}}{\mathrm{qSw}} \frac{5}{(0.5 \times 0.987 \times 10^2 \times 0.42)} = 0.2412$$

Putting values for $\mathrm{Cd_{LW}}$

$$\mathrm{Cd_{LW}} = \frac{\mathrm{Clw}^2}{\pi \mathrm{Ae}} + 0 + 0 = \frac{0.2412^2}{3.14 \times 7 \times 0.7875}$$

$$\mathrm{Cd_{LW}} = 0.0037$$

3.3 Total Wing drag

Total drag of the wing can be calculated as

$$\mathrm{Cd_W} = \mathrm{Cd_{oW}} + \mathrm{Cd_{LW}}$$

Putting the values calculated above,

$$\mathrm{Cd_W} = 0.0117 + 0.0037 = 0.0309$$

Since we are dealing with low subsonic mach no thus, wave drag and drag divergence are not considered in our calculations and the result is final

3.4 Fuselage drag coefficient prediction

The subsonic drag coefficient is found from

$$Cd_f = Cd_{0f} + Cd_{Lf}$$

3.5 Fuselage zero lift drag coefficient Cd_{of}

$$Cd_{0f} = R_{wf} Cf_{fuselage} \frac{\left\{1 + \frac{60}{\left(\frac{l_f}{d_f}\right)^3} + 0.0025\left(\frac{l_f}{d_f}\right)\right\} Swet_{fuselage}}{S} + Cd_{b\ fuselage}$$

Where,

To find R_{wf} need to find $Rn_{fuselage}$

$$Rn_{fuselage} = \frac{\rho U_1 l_f}{\mu}$$

We have at 1000ft altitude, density is 0.00217 slug/ft^{3}or 0.987kg/m^3,U=32.81ft/s, or 10m/sLf=1.7mor 5.57ft and Nu=1.11x10^{-5}Ns/m^2. Putting values in the above equation for the $Rn_{fuselage}$ we get,

$$Rn_{fuselage} = \frac{0.987 \times 10 \times 1.7}{1.22 \times 10^{-5}} = 1.3745 \times 10^6$$

R_{wf} Wing/fuselage interference factor = $1, d_f$ is the max fuselage diameter (0.192m), $Swet_{fuselage}$ wetted area if fuselage (0.834 m^2), $Cd_{b\ fuselage}$ fuselage base drag coefficient is given by

$$Cd_{b\ fuselage} = \frac{0.029\left(\frac{d_b}{d_f}\right)^3}{\sqrt{Cd_{0\ fus-base}(S_{wet}/S_{fus})}}(S_{fus}/S_{wet})$$

Where,S_{fus} is the maximum fuselage frontal area (0.127 x 0.199 = 0.02527 m^2) and S is the fuselage projected area 0.6045ft^2. Cf_{fus} is turbulent flat plate coefficient taken to be 0.0031

$d_b = \sqrt{\frac{4}{pi} x\ S_{fus}} = d_b = \sqrt{\frac{4}{3.14} x\ (0.127x0.199)} = 0.1794$, where the frontal area is 0.127m x 0.199m

$d_f = \sqrt{\frac{4}{pi} x\ S_{bfus}} = d_f = \sqrt{\frac{4}{pi} x\ S_{bfus}} = 0.066$ where fuselage base area is 0.05x0.07m=0.0035

$Cd_{0\ fus-base}$ zero lift drag coefficient of fuselage exclusive of base

$$Cd_{0f} = R_{wf} Cf_{fuselage} \left(1 + \frac{60}{\left(\frac{lf}{df}\right)^3}\right) + Cd_{b\ fuselage} = Cd_{0f}$$

$$= 1x0.0031 \left(1 + \frac{60}{\left(\frac{1.7}{0.066}\right)^3}\right) + Cd_{b\ fuselage}$$

$$Cd_{0f} = 0.0031 + Cd_{b\ fuselage}$$

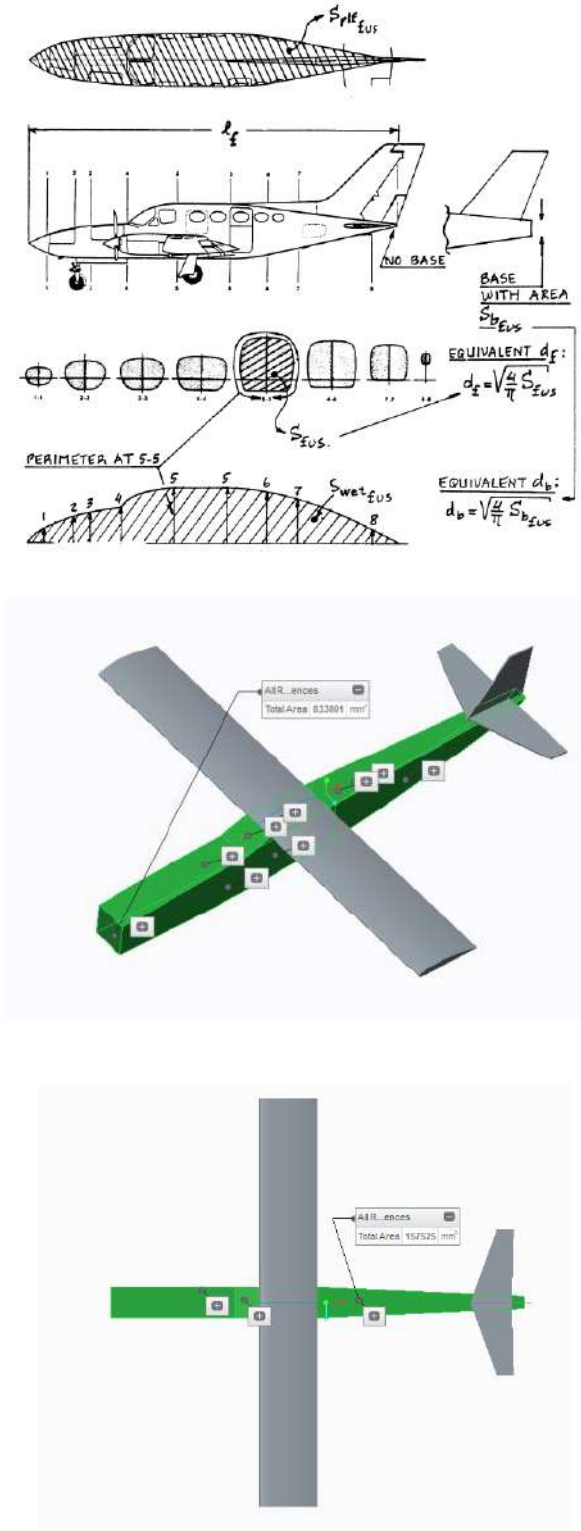

Figure 25 : Fuselage drag estimation guide (b) Wetted Area Calculation

S_{fus} is the maximum fuselage frontal area (0.199 x 0.127 = 0.0253m^2)and S is the fuselage projected area 157525mm^{2}or 0.1575m^2

$$Cd_{b\ fuselage} = \frac{0.029\left(\frac{d_b}{d_f}\right)^3}{\sqrt{Cd_{0\ fus-base}(S_{wet}/S_{fus})}}(S_{fus}/S_{wet})$$

$$Cd_{b\ fuselage} = \frac{0.029\left(\frac{0.1794}{0.066}\right)^3}{\sqrt{0.0031 \times \left(\frac{0.834}{0.0253}\right)}}\left(\frac{0.0253}{0.834}\right)$$

Calculating and putting all the values for $Cd_{b\ fuselage}$we get,

$$Cd_{b\ fuselage} = 0.0533$$

So the value of Cd_{0f} becomes

$$Cd_{0f} = 0.0031+0.0533$$

$$Cd_{0f} = 0.0564$$

3.6 Drag coefficient due to lift of fuselage C_{dlf}

It is given as

$$Cd_{Lf} = \frac{2\alpha^2 S_{b\ fus}}{S} + \eta\ Cd_c \alpha^3 S_{plf\ fus}/S$$

$S_{b\ fus}$ is the base area of fuselage calculated from creo = 0.05 x 0.07 = 0.0035m^2

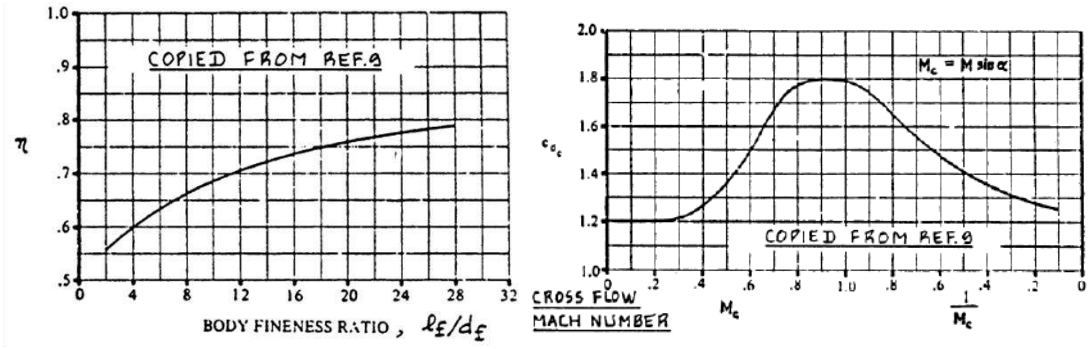

Figure 26 (a) Body Fineness Ratio Vs Etta (b) Cdc Vs Mach Critical

η is the ratio of drag of finite cylinder to infinite cylinder = 0.62 and $\mathrm{Cd_c} = 1.2$ (fig above). $S_{\mathrm{plf\ fus}}$ plan form area of the fuselagefrom Creo = 0.1575m^2 and α is fuselage angle of attack same as aircraft angle of attack given by

$$\alpha = \frac{\left(\frac{W}{\bar{q}S}\right) - \mathrm{Cl_0}}{\mathrm{Cl_\alpha}} = 0.03\ \mathrm{rad}$$

Putting all the values the Drag coefficient due to the lift of fuselage $\mathrm{Cd_{Lf}}$ becomes

$$\mathrm{Cd_{Lf}} = 0.000048$$

So, the total fuselage drag becomes,

$$\mathrm{Cd_f} = \mathrm{Cd_{0f}} + \mathrm{Cd_{Lf}} = 0.0564 + 0.000048 \ = 0.0564$$

3.7 Total Drag

$$\mathrm{C_D} = \mathrm{Cdo_{wing}} + \mathrm{Cdo_{fuselage}} + \mathrm{Cd_{Lwing}} + \mathrm{Cd_{Lfuselage}}$$

$$\mathrm{C_D} = 0.0117 + 0.0564 + 0.0037 + 0.000048$$

$$\mathrm{C_D} = 0.0681 + 0.003748$$

$$\mathrm{C_D} = 0.071848$$

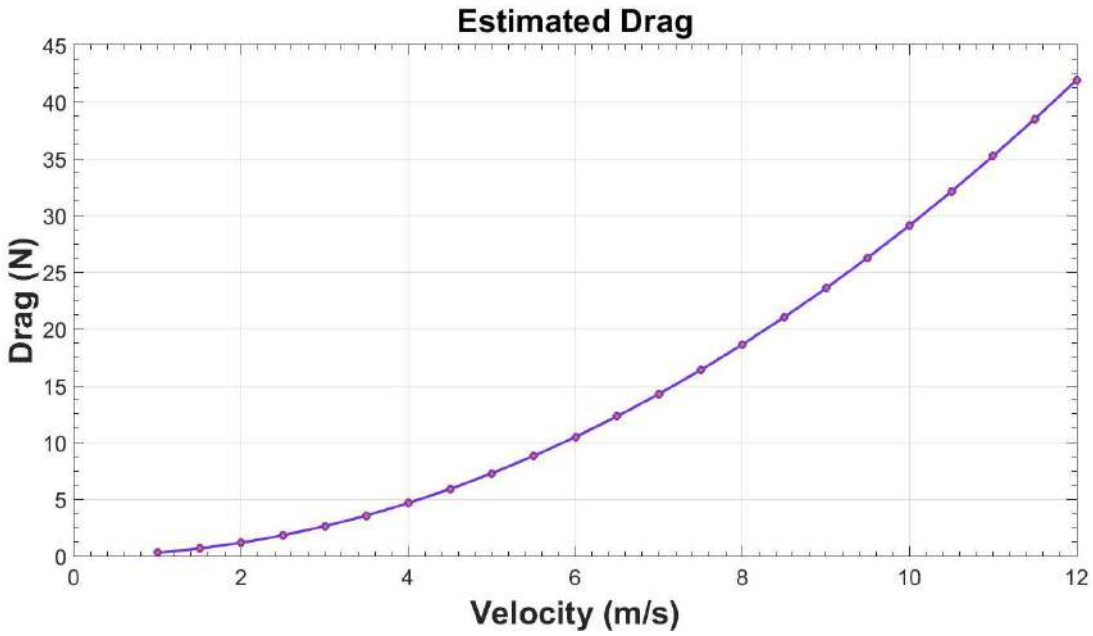

Figure 27: Velocity vs Drag

4 Propulsion Selection

4.1 Thrust Required (Drag) Curve

Following steps are involved in order to generate the Thrust required curve f

$$T_R = D = \frac{1}{2}\rho_\infty V_\infty^2 S C_D$$

But before proceeding, it is mandatory for us to know the value of drag polar i.e.

$$\boldsymbol{C_D = C_{Do} + KC_L^2}$$

Here $\mathbf{C_{D0}=0.0681}$**and** $\mathbf{C_L=0.0681}$while value of K is

$$\boldsymbol{K = k_1 + k_2 + k_3}$$

Where

k_1=Variation in parasite drag due to lift

k_2=Variation in wave drag due to lift

k_3=variation of drag due to finite wings

Here k_3 is given by

$$\boldsymbol{k_3 = \frac{1}{\pi . e . AR}}$$

This is the value of TR corresponding to the velocity chosen in step 1. This combination (TR, V∞) is one point on the thrust required curve

5. Repeat steps 1-4 for different values of V∞, thus generating enough points to plot the thrust required curve for UAV.

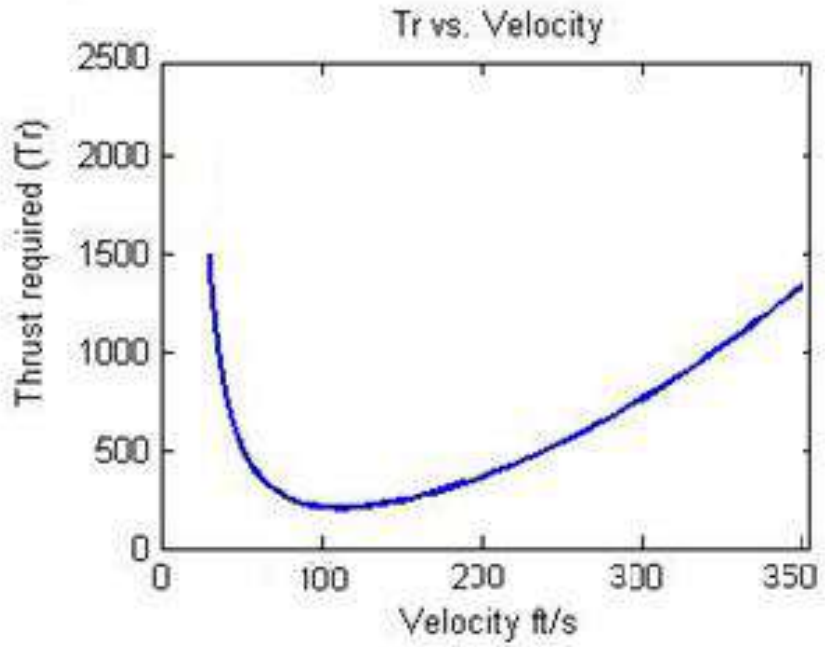

Figure 28: Thrust Required Vs Velocity

4.2 $T_{required}$ vs. $T_{available}$

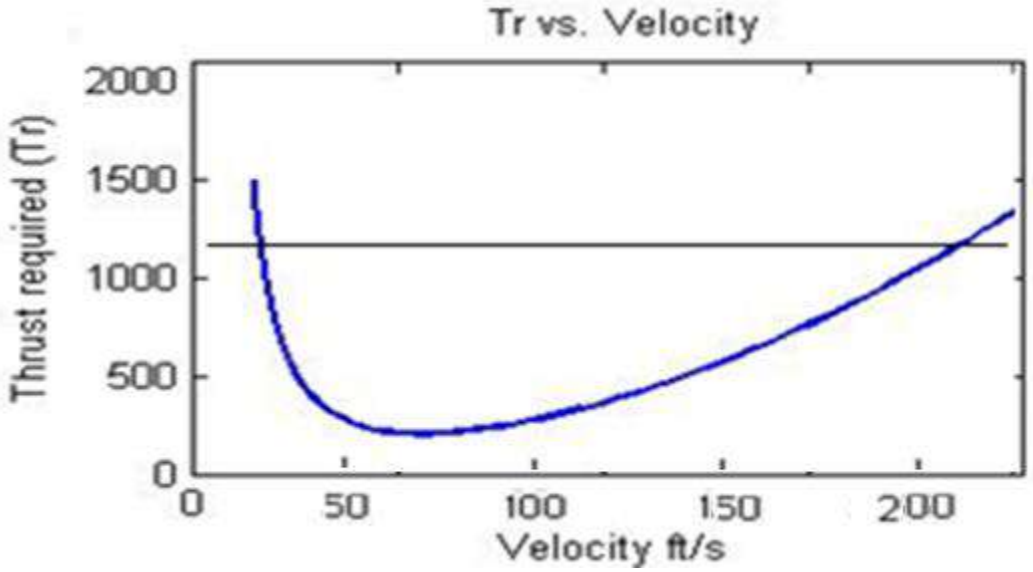

Figure 29: Thrust Required Vs Thrust Available

4.3 Drag Vs Velocity

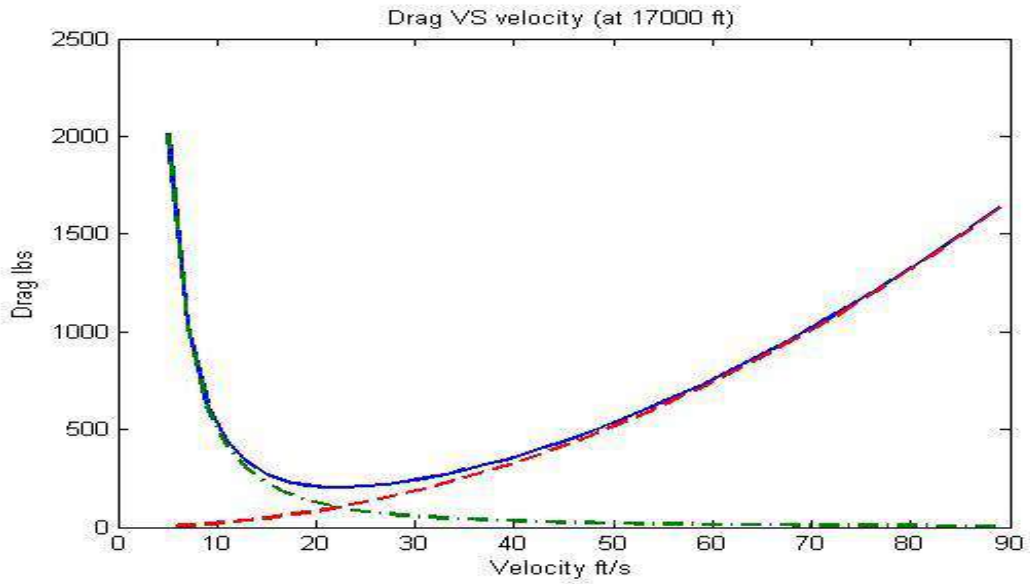

Figure 30: Drag Vs Velocity

4.4 L/D curve

(L/D) max is given by:

$$(L/D)_{max} = \frac{1}{\sqrt{4C_{D_o}K}}$$

Putting all the values we get

$$(L/D)_{max} = 18.1$$

This is same as shown in the graph

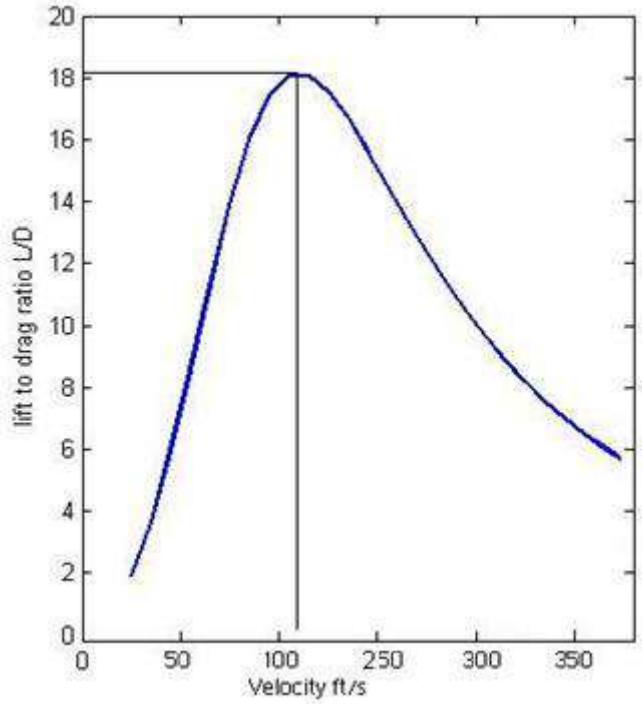

Figure 31: L by D curve

4.5 Power Available and Maximum Velocity

$$P_R = DV_\infty$$

$$D = q_\infty S C_D$$

$$C_D = C_{D_0} + K{C_L}^2$$

At cruise altitude;

$$C_{D_0} = 0.029$$

$$\rho = 0.001401 \text{ lb/ft}^3$$

$$S = 30.1 \text{ ft}^2$$

Power required can be calculated by simply multiplying thrust required, which is equal to drag in level and steady flight, with velocity. The plot of power required and power available vs. velocity is shown below.

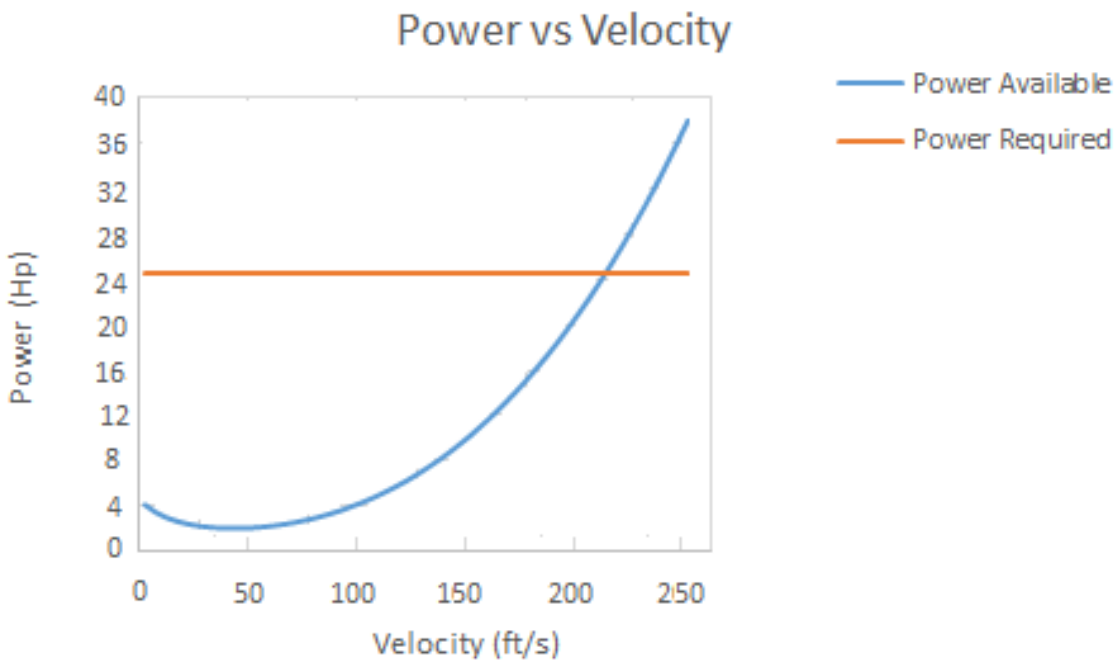

Figure 32 : Excess Power

The second intersection point corresponds to the maximum velocity of the aircraft, which in this case is approximately ft/s.

Generally in the analysis of airplane performance in the cruise range, it appears reasonable to assume thrust constant. Thrust Specific Fuel Consumption is also assumed to be constant with varying altitude and Mach numbers due to minor variation.

4.6 (ROC) Rate of Climb

Rate of climb is aircraft's vertical velocity- the rate of change in altitude. It depends upon the ratio of excess power to weight.

$$V_\infty \sin\theta = \frac{P_A - P_R}{W}$$

The difference between the two curves gives the value of excess power (T V_∞-D V_∞) at the corresponding point, we can obtain maximum rate of climb where this difference is maximum.

The graph of R/C vs velocity is shown below.

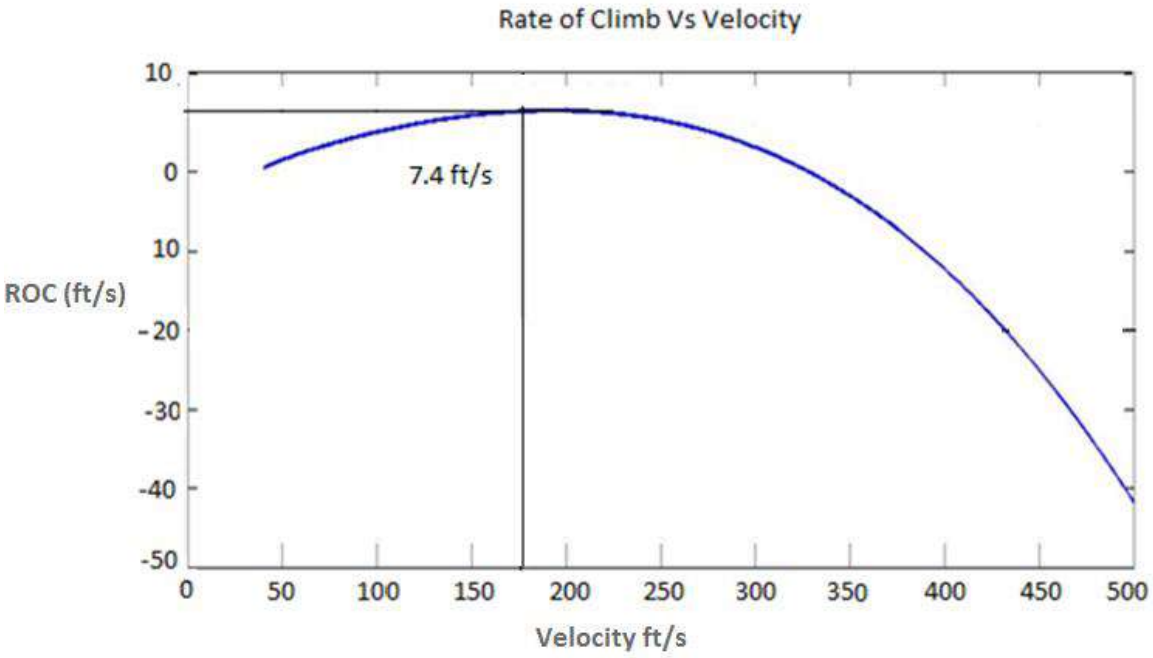

Figure 33: ROC

4.7 Takeoff Distance

Before calculating the takeoff distance we first calculate the maximum lift coefficient (C_{Lmax}), stall velocity (V_s) and thrust to weight ratio (T/W) for takeoff.

4.8 Maximum lift coefficient (C_{Lmax}):

C_{Lmax} is calculated from table

Table 8: Typical Values for High lift devices for takeoff and landing

Table 17.1: Typical values of high lift devices for landing and takeoff

High-Lift Device		Typical Flap Angle		$(C_L)_{max}/\cos \Lambda$	
Trailing Edge	**Leading Edge**	**Takeoff**	**Landing**	**Takeoff**	**Landing**
Plain flap		20°	60°	1.4–1.6	1.7–2.0
Single-slotted flap		20°	40°	1.5–1.7	1.8–2.2
Fowler flap					
single-slotted		15°	40°	2.0–2.2	2.5–2.9
double-slotted		20°	50°	1.7–1.95	2.3–2.7
double-slotted	slat	20°	50°	2.3–2.6	2.8–3.2
triple-slotted	slat	20°	40°	2.4–2.7	3.2–3.5

Plane flap was selected in Report 1, so for takeoff:

$$\frac{(C_L)_{max}}{\cos \Lambda} = 1.5$$

The quarter chord sweep angle calculated before was 6°, so:

$$\frac{(C_L)_{max}}{\cos 6°} = 1.5$$

$$(C_L)_{max} = 1.49$$

4.9 Stall velocity (V_s):

The stall velocity is calculated as:

$$V_s = \sqrt{\frac{2}{\rho_\infty}\frac{W}{S}\frac{1}{(C_L)_{max}}}$$

where;

$\rho = 2.377X10^{-3} slug/ft^3$ (at sea-level)

W/S = 17.79 (from Report 1)

$C_{Lmax} = 1.59$

$$V_s = \sqrt{\frac{2}{2.377 \times 10^{-3}} \times 17.79 \times \frac{1}{1.59}}$$

$$V_s = 86.3 ft/s$$

4.10 Thrust to weight ratio (T/W):

Since the engine proposed is the piston propeller driven, so we will convert horsepower to weight ratio (hp/W) into thrust to weight ratio (T/W) by using the following relation:

$$\frac{T}{W} = \frac{550 \eta_p}{V_\infty}\left(\frac{hp}{W}\right)$$

Where

$\eta_p = 0.8$ (from Report 1)

hp/W = 0.09853 (from Report 1)

V_∞ is calculated as:

$$V_\infty = 0.7V_{LO}$$

And V_{LO} for military aircraft is given by:

$$V_{LO} = 1.1V_s$$

V_s = 97.02ft/s (calculated above)

$$V_{LO} = 1.1 \times 86.3 = 95.01ft/s$$

So;

$$V_\infty = 0.7V_{LO} = 0.7 \times 95.01 = 66.5ft/s$$

Putting values we get:

$$\frac{T}{W} = \frac{550 \times 0.8}{66.5} \times 0.09853$$

$$\frac{T}{W} = 0.6518$$

Now, the total takeoff distance includes airborne distance and ground roll.

$$s_{TO} = s_a + s_g \quad \text{\_\_\_\_\_(17.1)}$$

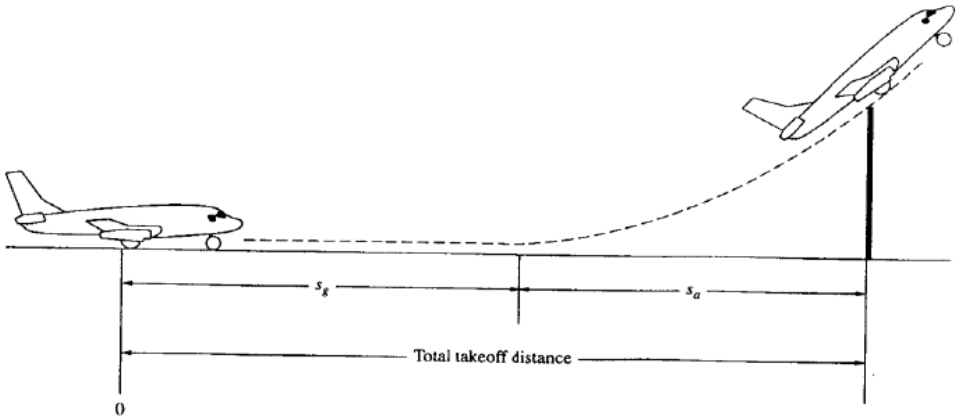

Figure 34: Illustration of ground roll S_g, airborne distance S_a, and total takeoff distance

The airborne distance is given by:

$$s_a = R \sin \theta_{OB} \quad \text{\_\_\_\_\_(17.2)}$$

Where

$$R = \frac{6.96(V_s)^2}{g}$$

V_s = 86.3ft/s

g = 32.2ft/s^2

$$R = \frac{6.96 \times (97.02)^2}{32.2}$$

$$R = 1609.8ft$$

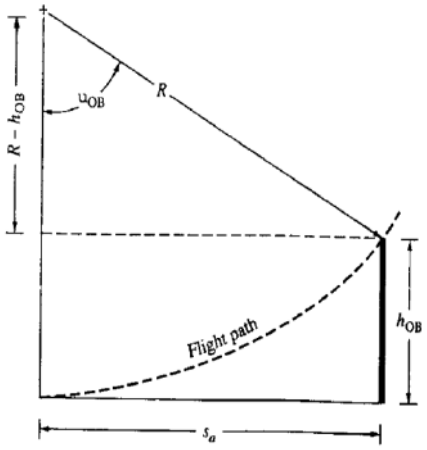

Figure 35: Sketch for the calculation of distance while airborne

And,

$$\theta_{OB} = \cos^{-1}\left(1 - \frac{h_{OB}}{R}\right)$$

h_{OB} = 50ft (assuming obstacle clearance height)

R = 2034.58ft

$$\theta_{OB} = \cos^{-1}\left(1 - \frac{15}{1609.8}\right)$$

$$\theta_{OB} = 7.82°$$

Putting values in Eqn. 17.2, we get:

$$s_a = 1069.8 \times \sin 7.82°$$

$$\boldsymbol{s_a = 220ft}$$

The approximate relation for ground roll is given by:

$$s_g = \frac{1.21\ W/S}{g\rho_\infty (C_L)_{max}\, T/W}$$

Where

g = 32.2ft/s^2

ρ = 2.377X10^{-3}slug/ft^3 (at sea-level)

T/W = 0.618 (calculated above)

$$s_g = \frac{1.21 \times 12.1}{32.2 \times 2.377 \times 10^{-3} \times 1.49 \times 0.6518}$$

$$\boldsymbol{s_g = 203.55ft}$$

Finally the total takeoff distance from Eqn. 17.1 is:

$$s_{TO} = s_a + s_g$$

$$s_{TO} = \mathbf{220 + 203.55}$$

$$\boldsymbol{s_{TO} = 424ft}$$

4.11 Landing Distance

Before calculating the landing distance we first calculate the maximum lift coefficient (C_{Lmax}), stall velocity (V_s) and thrust to weight ratio (T/W) for landing.

4.12 Maximum lift coefficient (C_{Lmax}):

C_{Lmax} is calculated from table 17.1 in the plane flap category for landing:

$$\frac{(C_L)_{max}}{\cos \Lambda} = 1.8$$

The quarter chord sweep angle calculated before was 6^o, so:

$$\frac{(C_L)_{max}}{\cos 6°} = 1.8$$

$$(C_L)_{max} = 1.79$$

4.13 Stall velocity (V_s):

The stall velocity is calculated as:

$$V_s = \sqrt{\frac{2}{\rho_\infty}\frac{W}{S}\frac{1}{(C_L)_{max}}}$$

Where

$\rho = 2.377X10^{-3}slug/ft^3$ (at sea-level)

W/S = 8.795 (from Report 1)

$C_{Lmax} = 1.79$

$$V_s = \sqrt{\frac{2}{2.377 \times 10^{-3}} \times 8.795 \times \frac{1}{1.79}}$$

$$V_s = 64.3\ ft/s$$

4.14 Thrust to weight ratio (T/W):

$$\frac{T}{W} = \frac{550\eta_p}{V_\infty}\left(\frac{hp}{W}\right)$$

Where

$\eta_p = 0.8$ (from Report 1)

hp/W = 0.063 (from Report 1)

V_∞ is calculated as:

$$V_\infty = 0.7V_{TD}$$

And V_{TO} for military aircraft is given by:

$$V_{TD} = 1.1V_s$$

V_s = 97.02ft/s (calculated above)

$$V_{TD} = 1.1 \times 64.3 = 70.8ft/s$$

So,

$$V_\infty = 0.7V_{TD} = 0.7 \times 70.8 = 49.5ft/s$$

Putting values we get:

$$\frac{T}{W} = \frac{550 \times 0.8}{49.5} \times 0.063$$

$$\frac{T}{W} = 0.5324$$

Now, the total landing distance includes approach distance, flare distance and ground roll.

$$s_L = s_a + s_f + s_g \quad \text{\_\_\_\_\_(17.3)}$$

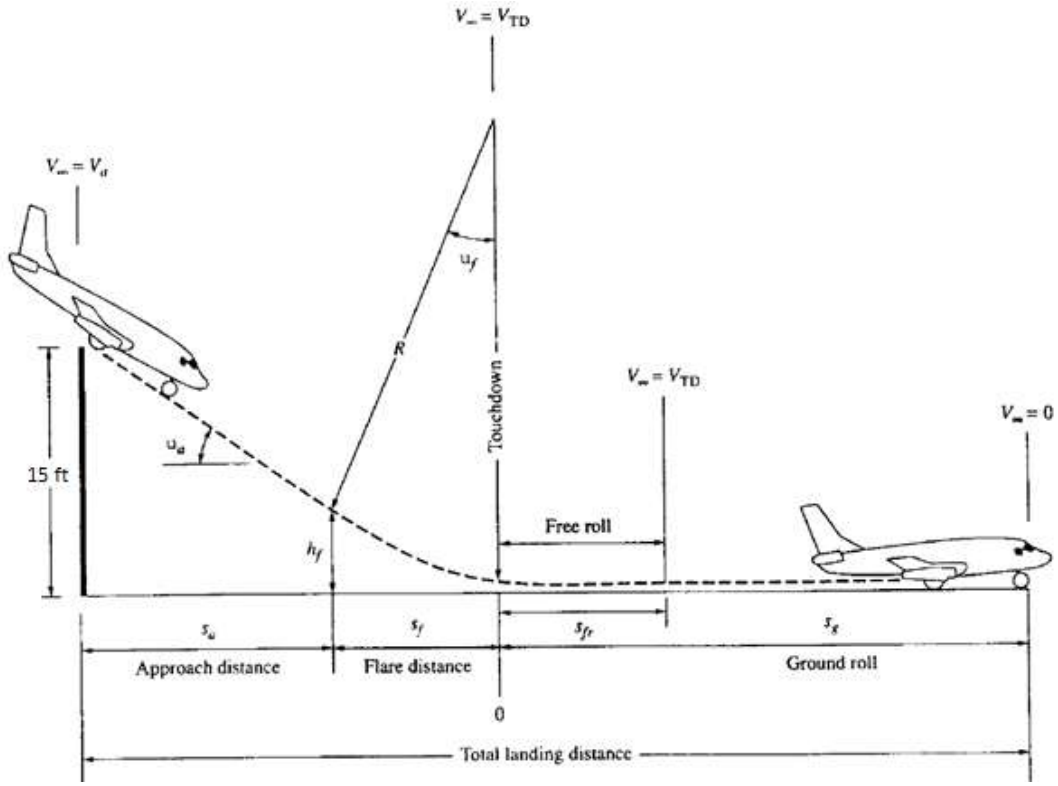

Figure 36: The landing path and landing distance

The approach distance is given by:

$$s_a = \frac{15 - h_f}{\tan \theta_a} \quad \text{\_\_\_\_\_(17.4)}$$

Where

$$h_f = R(1 - \cos \theta_a) \quad \text{\_\_\_\_\_(17.5)}$$

And

$$R = \frac{(V_f)^2}{0.2g} \quad \text{_____(17.6)}$$

The average flare velocity during flare for military aircraft is:

$$V_f = 1.15V_s$$

$$V_f = 1.15 \times 64.3 = 73.9ft/s$$

Eqn. 17.6 implies:

$$R = \frac{(99.72)^2}{0.2 \times 32.2}$$

$$R = 849.04ft$$

Assuming $\theta_a = 5^o$, Eqn. 17.5 implies:

$$h_f = 849.04 \times (1 - \cos 5°)$$

$$h_f = 3.23ft$$

Putting values in Eqn. 17.4 we get approach distance as:

$$s_a = \frac{15 - 5.87}{\tan 5°}$$

$$\boldsymbol{s_a = 104.3ft}$$

The flare distance is given by:

$$s_f = R \sin \theta_a$$

$$s_f = 849.04 \times \sin 5°$$

$$\boldsymbol{s_f = 73.99ft}$$

The approximate relation for ground roll is given by:

$$s_g = \frac{1.21\ W/S}{g\rho_\infty (C_L)_{max}\, T/W}$$

Where,

W/S = 8.795 (from Report 1)

C_{Lmax} = 1.7 (calculated above)

g = 32.2ft/s^2

ρ = 2.377X10^{-3}slug/ft^3 (at sea-level)

T/W = 0.5324 (calculated above)

$$s_g = \frac{1.21 \times 8.795}{32.2 \times 2.377 \times 10^{-3} \times 1.7 \times 0.5324}$$

$$\boldsymbol{s_g = 158.76ft}$$

Finally the total landing distance from Eqn. 17.3 is:

$$s_L = s_a + s_f + s_g$$

$$s_L = 104.3 + 73.99 + 158.76$$

$$\boldsymbol{s_L = 337.05ft}$$

4.15 Comparison of Performance Parameters

Parameters	Required	Calculated	Deviation
MTOW (lbs)	*350*	*386*	*10.2%*
Range (nm)	*370*	*349*	*5.6%*
Endurance (hrs)	*10*	*9.07*	*6.87%*
TO Distance(ft)	*500*	*423.5*	*12%*
Landing distance (ft)	*500*	*337.05*	*32.5%*

Table 9: Performance parameters comparison

4.16 Summary

Performance Analysis Summary	
Parameters	***Values***

Maximum lift to drag ratio $(L/D)_{max}$:	*18.1*
Velocity at maximum lift to drag ratio $(V_{L/D})_{max}$:	*117.9 ft/s*
Maximum rate of climb (ROC_{max}) :	*7.4ft/s*
Velocity at maximum rate of climb $(V_{ROC})_{max}$:	*180 ft/s*
Power available (P_A) :	*26 hp*
Maximum velocity (V_{max}) :	*256.7 ft/s*
Range:	*349 nm*
Endurance:	*11.2 hrs*
Takeoff distance :	*423.5 ft*
Landing distance :	*337.05 ft*

Table 10 Summary of Performance parameters

5 CFD ANALYSIS

Geometry was made using Creo 2.0 and later imported in ANSYS design modeler. The mesh was created using the ANSYS mesh module. The mesh is then imported to the fluent for numerical analysis. Below is the schematic for the whole process.

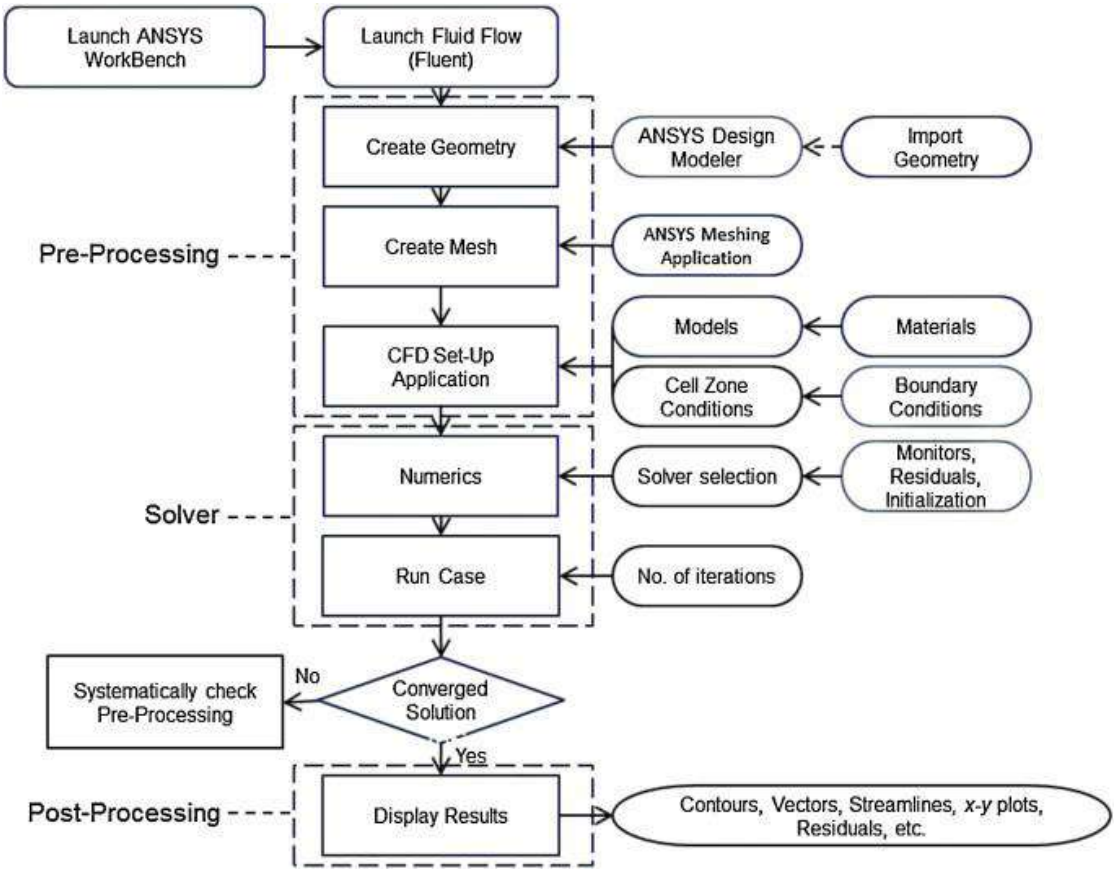

Figure 37: Schematic to carry out any CFD problem

5.1 Geometry

Isometric View geometry is shown in Figure 4.2 (a). It is a high wing aircraft.

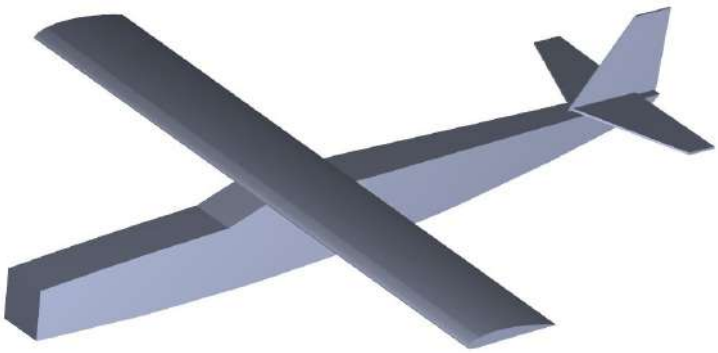

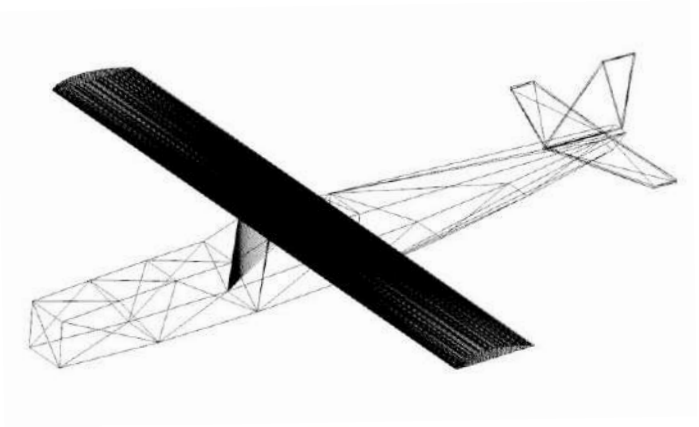

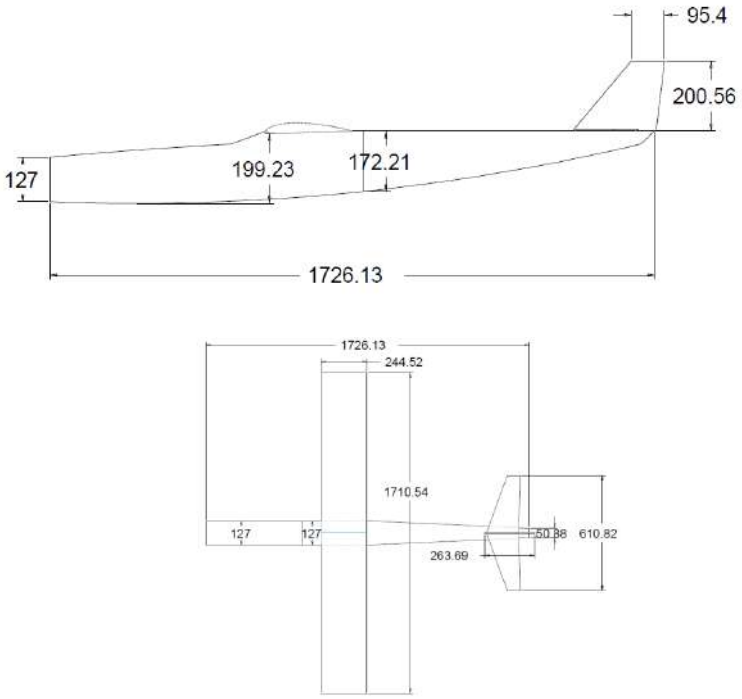

Figure 38: Views (a) Isometric (b) Top (c) Front (d) Span Wise Profile

5.2 Domain Size

When doing Meshing for CFD analysis, you should first determine the fluid domain. Upper and lower symmetry 5 x wing chord length is recommended. For 3D geometries, one is always concerned about the computational power. A rule of thumb never exists in such problems because unfortunately, everything is nonlinear. Experts recommend at least 5 times the reference length and reference length could be the wing chord, or Mean Aerodynamic chord for a good starting approximation. The domain size 16 x 8 x 5 m was finalized as shown in figure 4.3 (a & b).

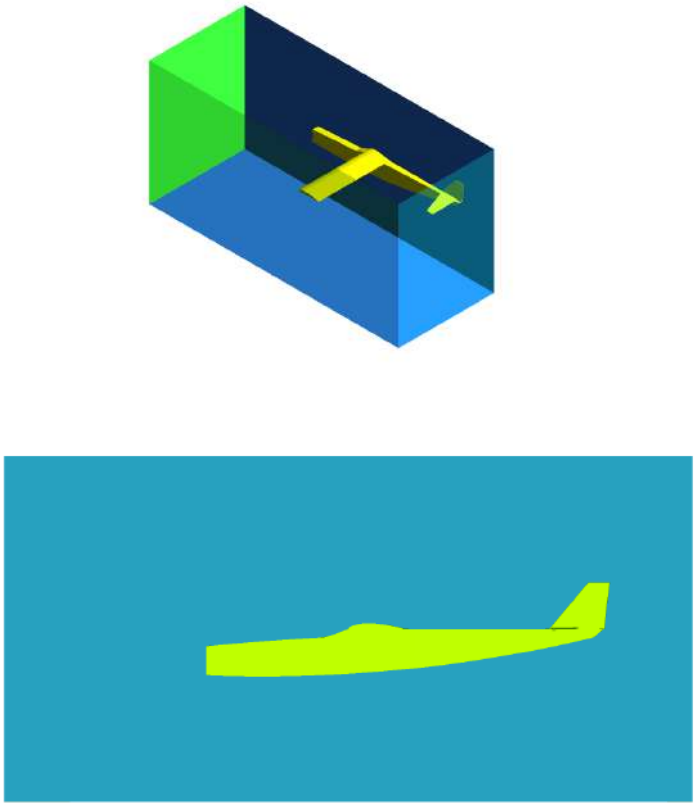

Figure 39: (a) 3D Domain, (b) Domain Size 2D

5.3 Meshing

Definition of the good mesh is a mesh which gives good accurate results and converges in the least possible time. It is important to locate the critical parts and area and refine only at some particular section of geometry, else mesh size will be reduced unnecessarily. Topology of the mesh is also an important factor to define the accuracy. For example, hexahedral geometry should be preferred over triangular or quadrilateral geometry for better accuracy. Mesh quality can be improved by using smoothening of mesh.

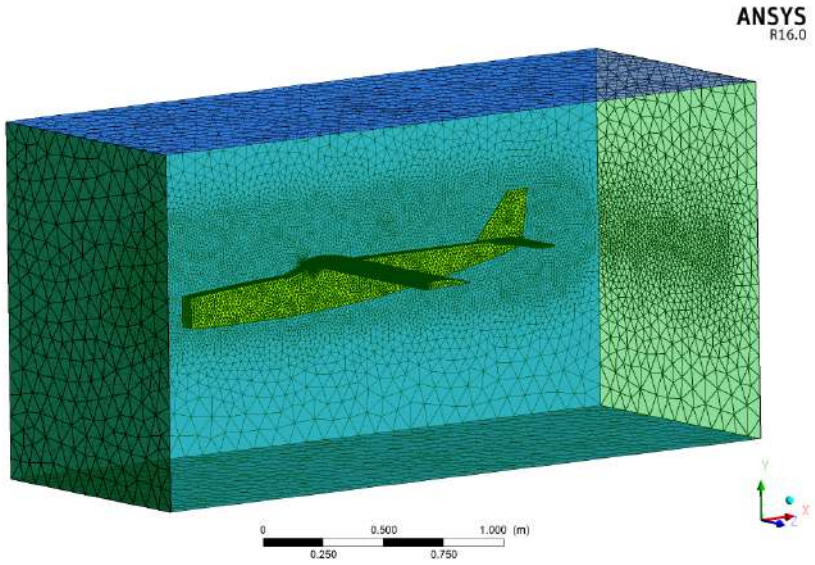

Figure 40: Mesh geometry in control volume

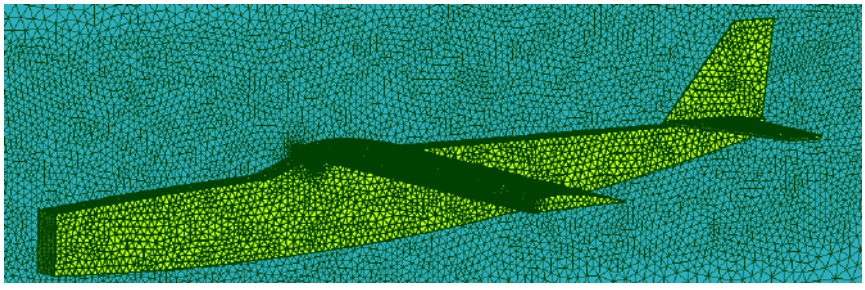

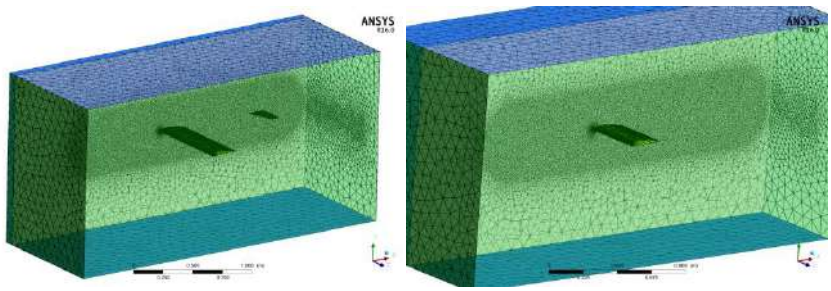

2. Mesh Report

Table 2. Mesh Information for FFF

Domain	Nodes	Elements
domain	618082	3616350

Figure 41 (a) Mesh Overview

5.4 Boundary Conditions

The outlet of the domain is specified as the as default outflow. The temperature (T), density (rho) and kinematic viscosity (μ) are taken from the standard atmosphere (ISA) and are 300K (ambient T), 1.225kg/m^3 and 1.7894×10^{-5} respectively.

Table 11 Operating Parameters (Boundary Conditions)

Inlet (Velocity m/s)		Outlet	Outflow
Upper, Lower, Left Far Field	Symmetry	Operating Pressure / Temperature	101325Pa / 300K
Fluid	Air (ideal)	Density	1.225kg/m^3
Reference Length	0.2m	Kinematic Viscosity	1.7894E-5kg/m.s

5.5 Results and Discussion

The lift, drag and moment coefficient has been evaluated and trends are presented in figure 4.7, 4.8 & 4.9. Figure 4.7 shows the Lift coefficient converged to 0.16.

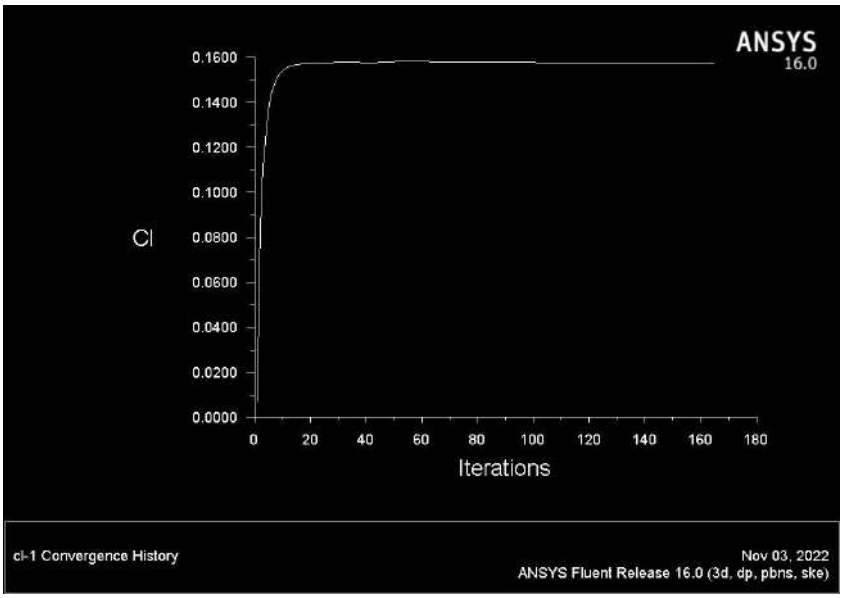

Figure 42 : (a) C_L at zero AOA (α)

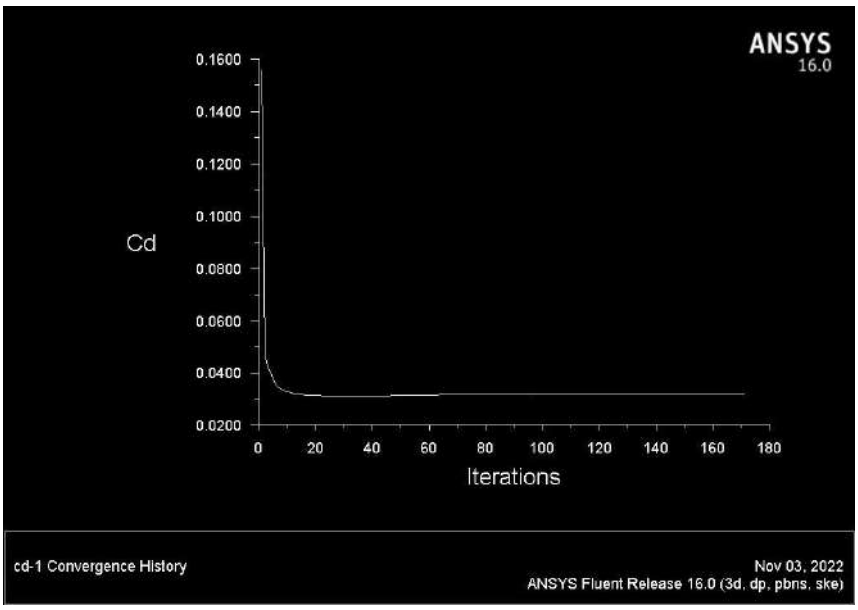

Figure 43 (a) C_D Vs Alpha (α

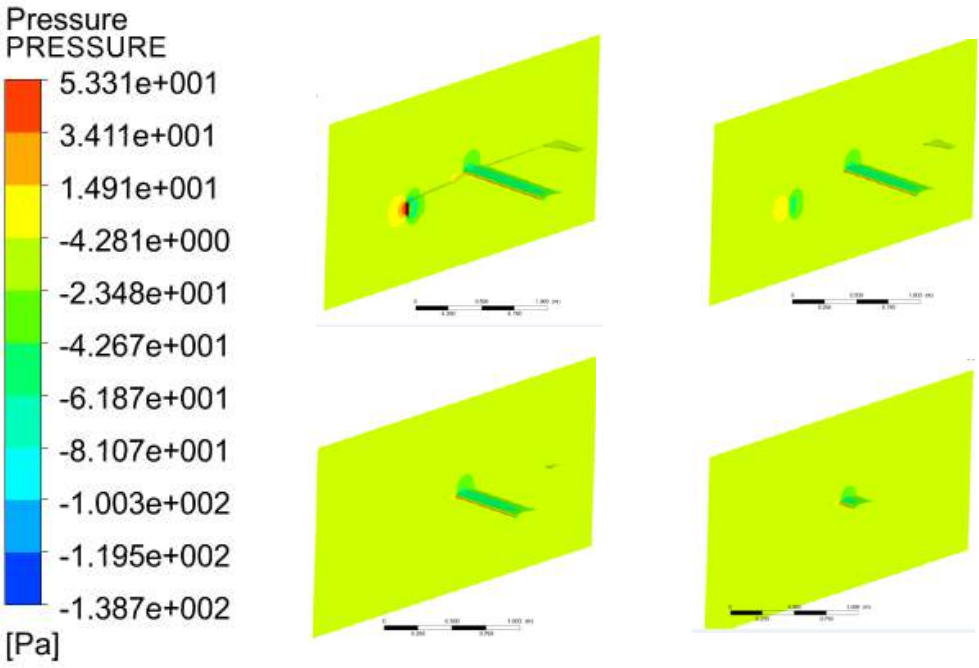

Figure 44: Pressure distribution on UAV

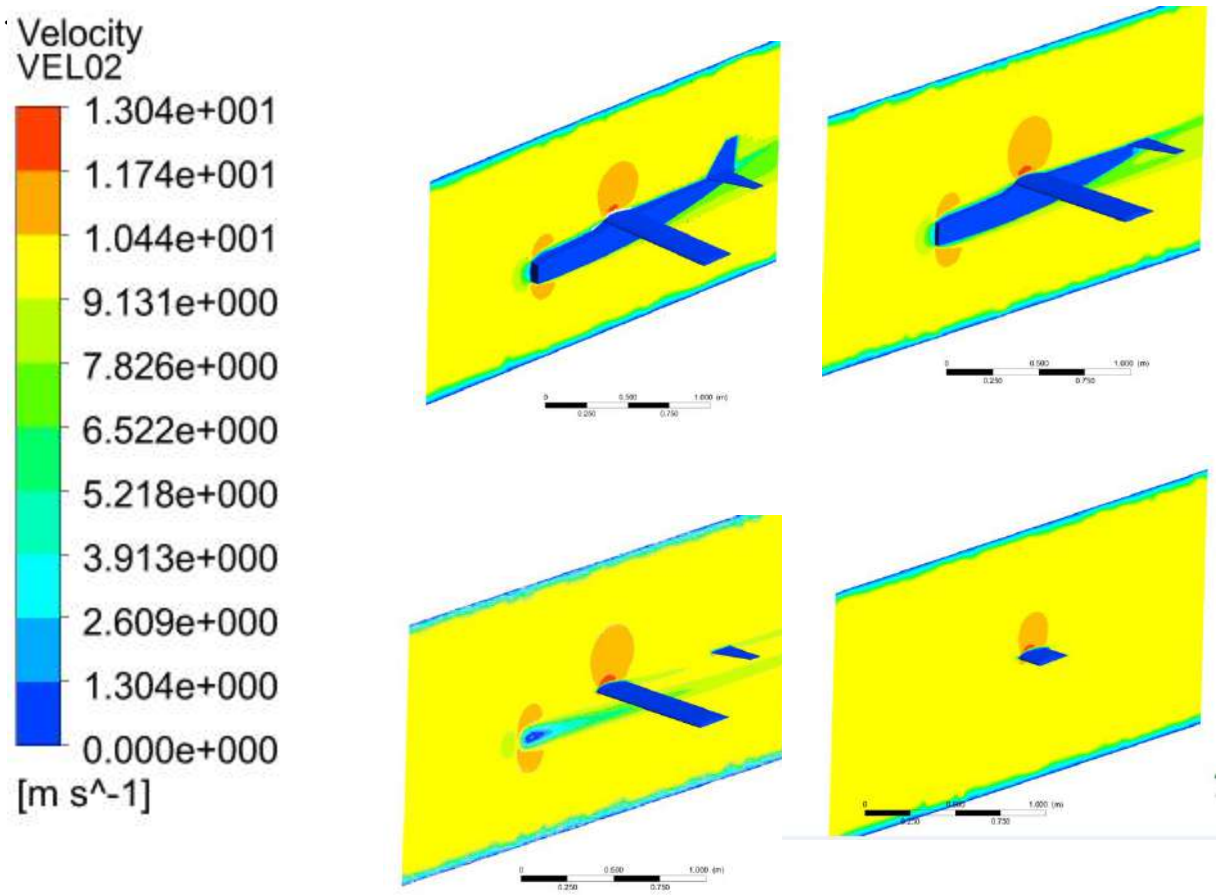

Figure 45: Velocity Distribution on UAV

5.6 Summary

CL and CD found using CFD is as follows:-

#	CL	CD
(a)	0.158	0.032

6 Appendix- 1: NACA 4412 Airfoil Coordinates

X	Y	Z
1	0.0013	0
0.95	0.0147	0
0.9	0.0271	0
0.8	0.0489	0
0.7	0.0669	0
0.6	0.0814	0
0.5	0.0919	0
0.4	0.098	0
0.3	0.0976	0
0.25	0.0941	0
0.2	0.088	0
0.15	0.0789	0
0.1	0.0659	0
0.075	0.0576	0
0.05	0.0473	0
0.025	0.0339	0
0.0125	0.0244	0
0	0	0
0.0125	-0.0143	0
0.025	-0.0195	0
0.05	-0.0249	0
0.075	-0.0274	0
0.1	-0.0286	0
0.15	-0.0288	0
0.2	-0.0274	0
0.25	-0.025	0
0.3	-0.0226	0
0.4	-0.018	0
0.5	-0.014	0

0.6	-0.01	0
0.7	-0.0065	0
0.8	-0.0039	0
0.9	-0.0022	0
0.95	-0.0016	0
1	-0.0013	0

6.1 Drawing Package

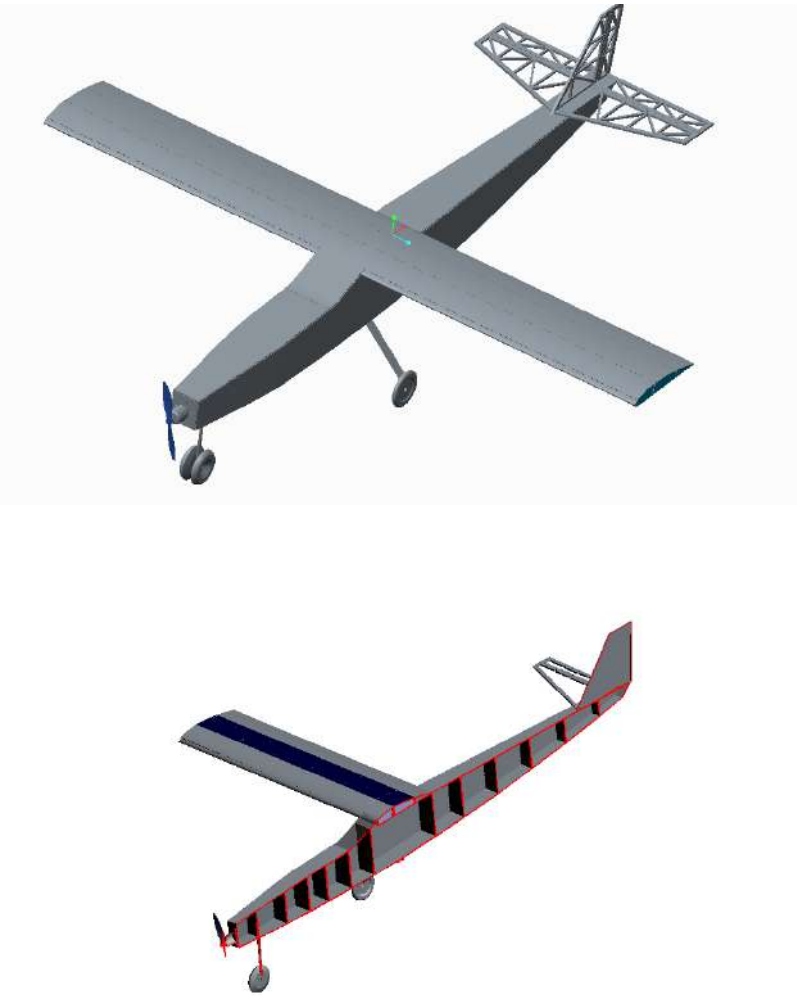

Figure 46: Model in Creo 2.0

This section gives a detailed overview of the dimensions and parameters of the aircraft.

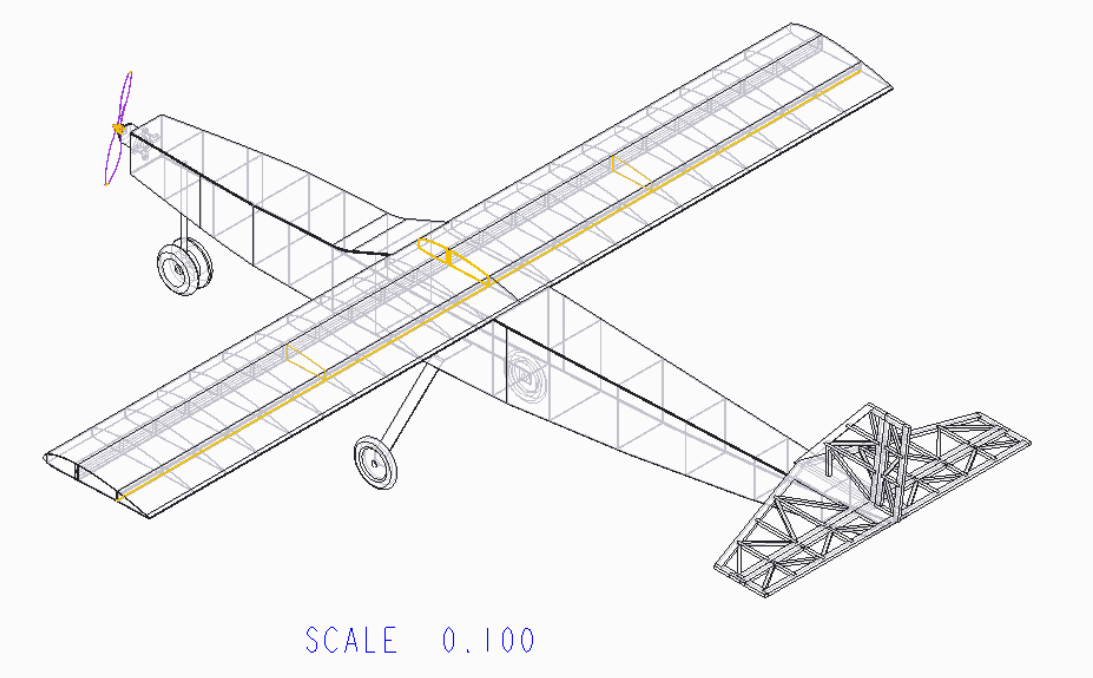

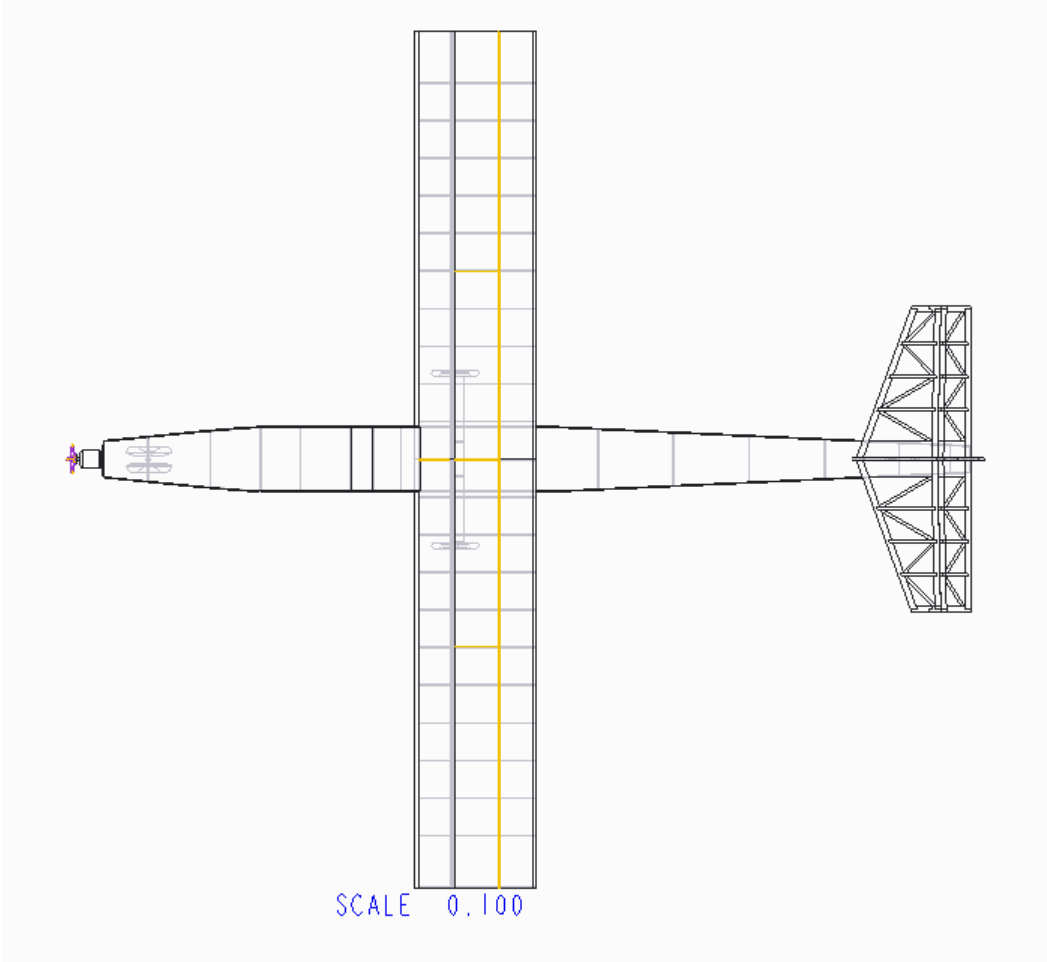

Figure 47: View Drawing with Dimensions

Figure 48: Exploded View of Structural Arrangements

All Dimensions are in mm.

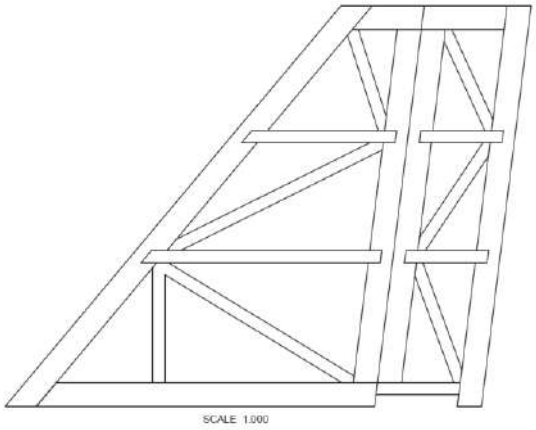

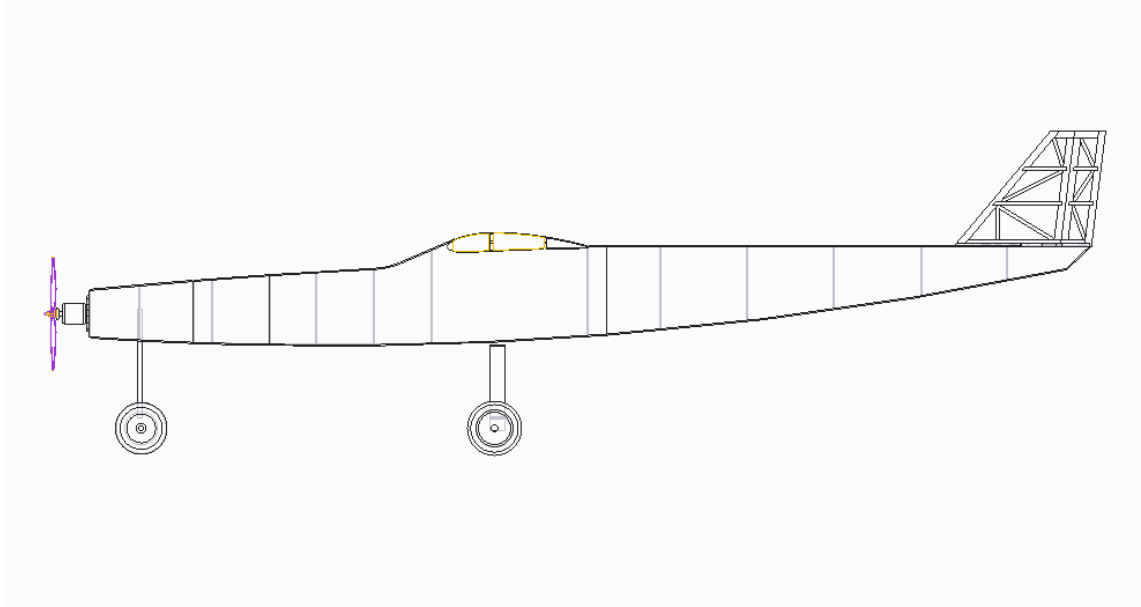

Figure 49: Systems Layout Drawing

7 Manufacturing Plans and Processes

Although the aircraft was sized to be as light as possible, multiple manufacturing methods were experimented with to conserve weight. Our manufacturing plan focused on the production of four main components: wing, landing gear, motor mount, and payload mount system

7.1 Manufacturing and Material Selection

- **Balsa**: This material can be very light and easy to form to different contours using cutters. Depending on where it is used, balsa is a reinforcing material and is a good material to use in terms of less weight. Balsa wood increases shear strength as well as bending modes when combined to weak structures.
- **Carbon Fiber**: Carbon fiber is a lightweight fiber used in advanced composites. This material is manufactured by utilizing a wet layup process where carbon fiber cloth is placed over a mold with resin distributed along the surface area, and then vacuum bagged and cured. Different orientations of weaving patterns will increase the shear strength and bending stiffness.
- **Plywood**: Plywood is a laminated product made up of numerous thin strips of wood laid in alternating directions and bonded with glue into strong, stable sheets which provide high stiffness and strengths.
- **Aluminum:** This material is a highly diverse element which can be molded into different shapes. Aluminum is strong in tension and compression, but if used too much it will add extra unnecessary weight.
- **Epoxy:** It is a thermosetting resin used chiefly in strong adhesives and coatings and is used in the joining of two or more parts.
- **Brass:** It is an alloy of copper and zinc and is harder as compared to aluminum. It can take continuous cyclic loading without being deformed.
- **German Glue:** White Glue best used to join woods but it takes a long time to harden.

- **Elfy:** A strong adhesive used to join two materials permanently in minutes but makes the Balsa brittle.

For each major section of the airplane a FOM analysis was carried out in order to select the ideal material. The FOM analysis for each section had the same 4 parameters which were considered important by the team.

Weight: As the most important element it was necessary to select a material that reduced as much weight as possible wherever possible.

Strength: Although weight is the highest priority, if the structure can't handle the loads the aircraft will fail. The selected material must have a balance of weight and strength.

Manufacturability: A material that is quick and easy to manufacture is desired in case there is an unexpected failure of a part during the competition.

Cost: The material should not be too expensive.

Figures of Merit	Weight	Balsa	Plywood	Carbon Fiber
Weight	0.5	5	3	4
Strength	0.3	3	4	5
Manufacturability	0.15	5	4	1
Cost	0.05	5	4	1
Total	1.00	4.4	3.5	3.7

Table 12: Airfoil, Wing and Empennage Material Selection FOM Analysis

Figures of Merit	Weight	Balsa	Plywood	Carbon Fiber
Weight	0.2	5	3	3
Strength	0.6	3	4	5
Manufacturability	0.15	5	4	1
Cost	0.05	5	4	0
Total	1.00	3.8	3.8	3.75

Table 13: Fuselage Material Selection FOM Analysis

Figures of Merit	Weight	Brass	Aluminum	Carbon Fiber
Weight	0.1	3	5	5
Strength	0.6	4	3	5
Manufacturability	0.05	5	4	3
Cost	0.25	3	5	3
Total	1.00	3.7	3.75	4.40

Table 14: Landing Gear Material Selection FOM Analysis

Figures of Merit	Weight	Brass	Aluminum	Carbon Fiber
Weight	0.1	3	4	5
Strength	0.65	5	3	2
Cost	0.25	3	4	1
Total	1.00	4.3	3.35	2.05

Table 15: Gear Material Selection FOM Analysis

7.2 Aircraft Manufacturing Process

7.2.1 Wing, Empennage and Fuselage Manufacturing

First, the AutoCAD to the scale drawing was printed from a graph plotter. The airfoils were cut out and pasted on plywood to create a template. Then, using a combination of the cutter and the sanding machine, the airfoil template was cut out. Using that template, a series of airfoils was cut from 1/16 in Balsa sheet. After this, the plan of the wing was carefully pasted on the part of the table which was completely flat to avoid and abnormalities. After that a plastic sheet was used to cover the plan so that garbage does not get stuck from the leftover glue. Then, the required length of spar was cut and attached on the sheet. The airfoils were placed on the spar and were glued using elfy. Similarly, the rest of the components of the wing such as webs, leading edge spar, covering were cut out using cutters and sanded and attached.

The area which needed high strength of attachment (the area where the booms were to be inserted) was attached with epoxy. In most areas where we had to reduce weight from the adhesive as well as avoid making the wood brittle, German glue was used.

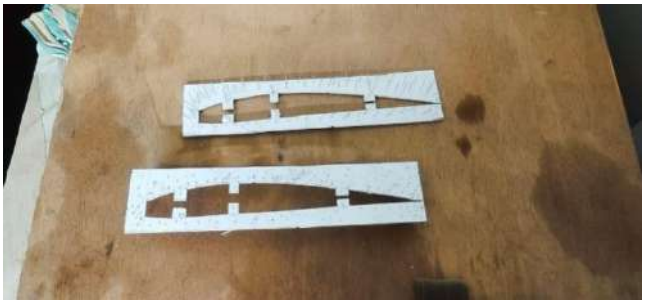

Figure 50: Cutting Out Airfoils Using the Template

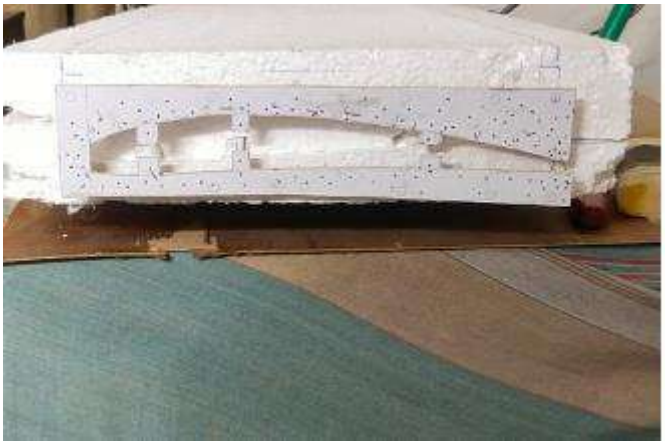

A total of 210 hrs consumed till finished product. All the items/processes followed are mentioned below.

Item / Process	Skill Req.	Qty.	Time Cons. (hrs)
Plan Making in Creo 2.0	3D Modeling /Drafting	01	18
Material Estimation	Drawing Reading	-	5
Procurement	Market survey	-	8
Cutting Airfoil Template -1 (wing side view)	Cutting / Filing Sanding	02	2
Cutting Airfoil Template -1 (wing side view)		04	2
Gluing 2" by 1x1m Styrofoam sheet		02	02
Fixing Template to Styrofoam Block	Precise Alignment / Hammering	06	18
Hot Wire Cutting of Views		03	5
Initial Profile Sanding	Sanding / Filing	-	4
Fine Sanding			12
Grooves for Fiberglass/ply strengthening layup	Cutting / Filing		1
Placement / Cutting Strips for reinforcement		-	4
Applying glue			3
Manufacturing of attachment adapters	Milling/drilling / Lathe	03	5
Attachment of Adapters	Fabrication		5
Joining of wing	fabrication		8

Manufacturing of H tail and VTail	Fabrication layout method		7
Manufacturing fuselage			8
Fixing of V-tail in the Model	Alignment		3
Fixing of h tail in the fuselage	Sanding	-	15
Covering	Sanding		68
Landing gear attachment	Spray Paint		3
Electronics attachment	Cutting		4

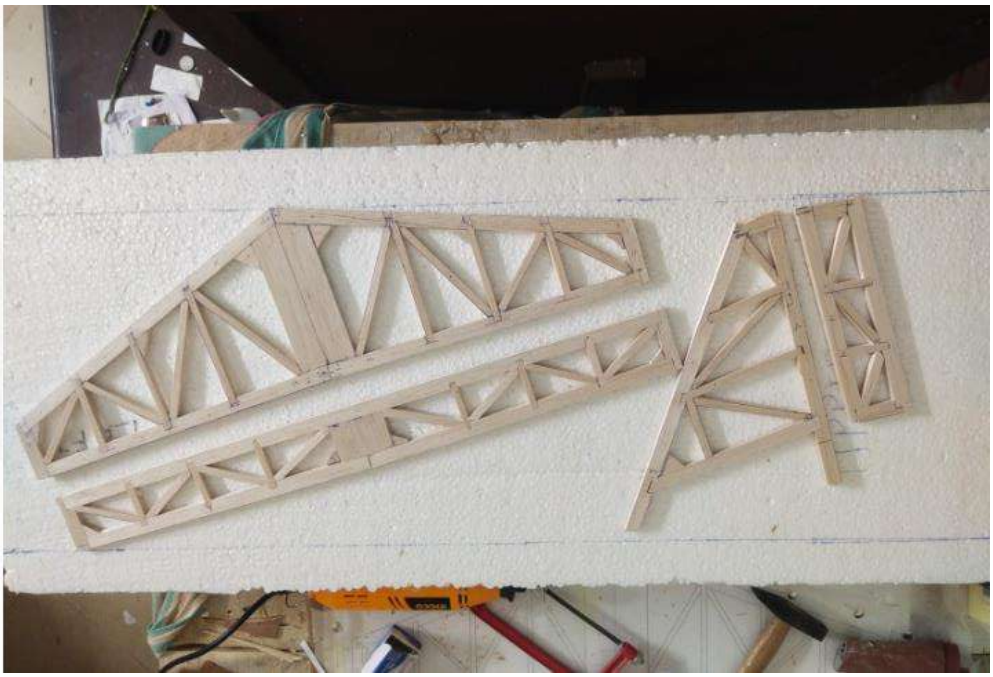

Figure 51: Wing, Tail and fuselage structure

The Fuselage plan was first traced on a sheet of plywood and then using the electric saw, the required portion was cut and hand sanded to make it smooth. Using the same piece, another similar piece was cut using the cutter and both were attached together using thumb pins. They were again sanded together to maintain equality. Blocks and bulkhead slots were removed from both of them together to maintain symmetry. They were then separated and joined together by using German glue and the Bulkheads.

Figure 52: Assembled Fuselage

Figure 53: Assembled Fuselage, Tail and Wing

7.3 Summary and feasibility study of possible manufacturing processes

Like the assortment of flying vehicles, there was an array of building materials that could be used to manufacture the aircraft. We resorted to a simple figure of merit test to narrow our choices, which predominantly had to do with previous knowledge and/or experience with or about the use of the material. For the test, any other factor such as weight, strength or time was ignored for the initial part.

A short table was constructed awarding points to categories of material that best fitted manufacturing the designed aircraft.

Skill	Wood-working	Foam Hotwiring	Molded Construction	Metal Working
Number of Personnel with Experience	5	2	1	3
Score	1	1	-1	0

Table 16

Landing gear

A detachable tri-cycle landing gear arrangement with single servo control for steering was selected, after reviewing structural failures on a similar body design supported by quadric-cycle landing gear mechanism. It comprised of

— one nose-wheel

— two side-wheels

with each wheel/gear being independent of the other.

Vertical tail

Simple balsa sheets were decided for the vertical tail assembly, without much internal structuring, keeping weight of the assembly as low as possible.

8 Final Product

9 Flight Sorties and Trials:

Figure 54: UAV Takeoff

Figure 55: UAV Flying in Air

10 Conclusion

As modern UAVs have grown significant research and development interest, much more research papers and scientific articles are being published. The rapidly increasing R&D of UAVs is a consequence of these advancements. Moreover, the demand for increased mobility, more autonomy and higher range of UAVs resulted in the design of novel systems for battery swapping, multi-stations and precision landing. The application of these is being used in surveillance, security, tracking, agriculture, for fire detection and prevention, disaster monitoring, wireless communication, remote sensing, monitoring, and highway traffic control etc. In this regard, efforts have been made to develop a prototype model. Parameters calculated from Mathematical model are used as input for finalization of geometry design. The model has been validated through CFD analysis. UAV model has been manufactured, developed and resulted in successful aerial test flight. Way forward in this area research includes the innovation and further testing /evaluation to accommodate weapons, night vision payload for military use.